Nano Today 36 (2021) 101052

Contents lists available at ScienceDirect

Nano Today

journal homepage: www.elsevier.com/locate/nanotoday

Review

What NIR photodynamic activation offers molecular targeted nanomedicines: Perspectives into the conundrum of tumor specificity and selectivity

Chanda Bhandari[a,1], Mina Guirguis[a,1], N. Anna Savan[b], Navadeep Shrivastava[a], Sabrina Oliveira[c,d], Tayyaba Hasan[e,f], Girgis Obaid[a,*]

[a] Department of Bioengineering, University of Texas at Dallas, Richardson, TX 75080, USA
[b] Michigan State University, East Lansing, MI 48824, USA
[c] Cell Biology, Neurobiology and Biophysics, Department of Biology, Science Faculty, Utrecht University, Utrecht 3584 CH, The Netherlands
[d] Pharmaceutics, Department of Pharmaceutical Sciences, Science Faculty, Utrecht University, Utrecht 3584 CG, The Netherlands
[e] Wellman Center for Photomedicine, Massachusetts General Hospital and Harvard Medical School, Boston, MA 02114, USA
[f] Division of Health Sciences and Technology, Harvard University and Massachusetts Institute of Technology, Cambridge, MA 02139, USA

ARTICLE INFO

Article history:
Received 24 August 2020
Received in revised form 2 November 2020
Accepted 2 December 2020
Available online 16 December 2020

Keywords:
Photodynamic therapy
Photonanomedicines
Specificity
Selectivity
Solid tumors

ABSTRACT

Near infrared (NIR) photodynamic activation is playing increasingly critical roles in cutting-edge anti-cancer nanomedicines, which include spatiotemporal control over induction of therapy, photodynamic priming, and phototriggered immunotherapy. Molecular targeted photonanomedicines (mt-PNMs) are tumor-specific nanoscale drug delivery systems, which capitalize on the unparalleled spatio-temporal precision of NIR photodynamic activation to augment the accuracy of tumor tissue treatment. mt-PNMs are emerging as a paradigm approach for the targeted treatment of solid tumors, yet remain highly complex and multifaceted. While ligand targeted nanomedicines in general suffer from interdependent challenges in biophysics, surface chemistry and nanotechnology, mt-PNMs provide distinct opportunities to synergistically potentiate the effects of ligand targeting. This review provides what we believe to be a much-need demarcation between the processes involved in *tumor specificity* (biomolecular recognition events) and *tumor selectivity* (preferential tumor accumulation) of ligand targeted nanomedicines, such as mt-PNMs, and elaborate on what NIR photodynamic activation has to offer. We discuss the interplay between both tumor specificity and tumor selectivity and the degree to which both may play central roles in cutting-edge NIR photoactivable nanotechnologies. A special emphasis is made on NIR photoactivable biomimetic nanotechnologies that capitalize on both specificity and selectivity phenomena to augment the safety and efficacy of photodynamic anti-tumor regimens.

Contents

Abbreviations: AlPcS4, Aluminum phthalocyanine tetra sulfate; AUC, Area Under Curve; BP, Bispyrene; CA, Cholic Acid; CD, Carbon nanodots; Ce6, Chlorine e6; Cet-PIN, Cetuximab Photoimmunonanoconjugate; EGFR, Epidermal Growth Factor Receptor; EPR, Enhanced Permeability and Retention (effect); FA, Folic Acid; FDG, 2′-deoxy-2′-(^{18}F) fluoro-D-glucose; FR, Folic Acid Receptor; HANP, Hyaluronic Acid Nanoparticles; HER-2, Human Epidermal Growth Factor Receptor-2; IC_{50}, Half Maximal Inhibitory Concentration; ICGD, Indocyanine Green Derivatives; IgG, Immunoglobulin G; LTN, Ligand Targeted Nanomedicines; mt-PNM, Molecular Targeted Photonanomedicines; MPS, Mononuclear Phagocytic System; NMOF, Nanoscale Metal Organic Framework; OAUCNP, Oleic Acid Upconversion Nanoparticles; PDT, Photodynamic Therapy; PDX, Patient-Derived Xenograft; PEG, Polyethylene Glycol; PIC, Photoimmunonanoconjugates; PS, Photosensitizer; PSMA, Prostate Specific Membrane Antigen; PTK7, Protein Tyrosine Kinase; RMS, Reactive Molecular Species; TAM, Tumor Associated Macrophages; ZnPC, Zinc(II)phthalocyanine

* Corresponding author.
E-mail address: Girgis.Obaid@utdallas.edu (G. Obaid).
[1] Both authors contributed equally to this study.

https://doi.org/10.1016/j.nantod.2020.101052
1748-0132/

Selectivity and specificity at the nanoscale for photodynamic therapy

NIR-activable photonanomedicines

Photodynamic therapy (PDT), a treatment modality capitalizing on photo-generated reactive molecular species (RMS), has seen a marked increase in use for an array of nanotechnology approaches in recent years [1]. Salient features of PDT-activated nanomedicines (photonanomedicines; PNMs) that have led to their recent widespread use include 1) unparalleled spatiotemporal control over activation and 2) simultaneous photochemical tumor tissue priming, damage and immunogenic cell death. Recent approaches that have capitalized on the unique features of NIR-responsive PNMs range from photochemically-triggered release of biologics [2,3], small molecule inhibitors [4], chemotherapeutics [5–10], and immunotherapeutics [11–14], in addition to various combinations of these agents. The specific importance of NIR light used for the photodynamic activation of PNMs is discussed in more detail in section *Distinctive advantages of NIR light activation.* As a result of the versatility and utility of NIR-activable PNMs for multimodal cancer imaging and therapeutics, targeting using ligand functionalization of various PNM formats is widely adopted to prepare molecular targeted (mt)-PNMs with the goal of achieving tumor-tissue specific treatment. The challenges and, more importantly, the distinctive advantages of NIR photoactivable mt-PNMs will be the focus of this review, with a specific emphasis made on the parallels between tumor specificity and tumor selectivity.

Defining specificity and selectivity: beyond semantics

Ligand targeted nanomedicines (LTNs; molecular targeted nanoscale drug delivery systems including nanoparticles, nanocomplexes and nanovesicles), naturally emerged from the understanding that dynamic molecular changes on the surface of cancer cells could distinguish them from healthy tissue, and could thus facilitate tumor-specific delivery of various nanomedicines. These changes are mostly associated with the over-expression of cognate receptors involved in survival and growth-related signaling cascades. The advent of bioengineered recognition molecules, referred to as targeting ligands in this review, formed the basis of targeted antibody therapeutics of which many are currently in mainstream oncological clinical practice. While conceptually attractive, fabricating universally reproducible and functionally viable LTNs that entrap high agent payloads is proving to be a significant challenge. Furthermore, the added biophysical complexity of photosensitizer (PS) molecules that serve as the activating agent and the primary therapeutic agent of mt-PNMs further propagates these challenges. Ultimately, the challenges stem from broad overgeneralizations, which assume that ligand conjugation will systematically improve mt-PNM phototherapeutic outcomes, whilst little conceptual differentiation between PNM *selectivity* and *specificity in vivo* is made. As such, it becomes critical to delineate between the two concepts in order to better define the pathophysiological consequences of ligand targeting prior to interpreting its outcomes.

Generally speaking, tumor *selectivity* is the phenomenon by which nanomedicines exhibit preferential delivery and accumulation in solid tumors as a function of disrupted vascular systems and interstitial fluid dynamics in a process widely referred to as the enhanced permeability and retention (EPR) effect [15]. *Specificity*, however, refers to the phenomenon by which LTNs, such as mt-PNMs, exhibit a discrete molecular affinity for tumor-associated molecular targets, thereby influencing cellular partitioning within the tumor interstitium at the nm–μm scale (Fig. 1).

Within the field of nanomedicine, the terms “selectivity” and “specificity” tend to be used loosely and interchangeably. While both phenomena are desirable, and to some extent can be interdependent, they are not synonymous. This is particularly problematic when the expected outcome of mt-PNM target biorecognition *in vivo* is often assumed to be an increase in tumor selective delivery, while their molecular specificity remains undermined and ambiguous. This is corroborated by the notion that molecular specificity can (not always) impact tumor selective delivery, while tumor selective delivery has no bearing on the molecular recognition processes that confer specificity. To further complicate matters, the use of the terms *passive targeting* (selectivity-based phenomenon) and *active targeting (*selectivity and specificity-based phenomenon) is widespread in the literature. While active targeting aims to achieve ligand-receptor recognition *in vivo,* the terminology does little to distinguish between tumor selective delivery and tumor specificity of mt-PNMs; and hence the existence of the conundrum. It is important to note here that while intertumoral and intratumoral receptor heterogeneity is a limitation for tumor specificity of mt-PNMs, intertumoral and intratumoral vascular heterogeneity in the EPR effect is a significant limitation for the tumor selective delivery and retention of mt-PNMs [16,17]. Vascular heterogeneity also exists between tumors arising in different organs and

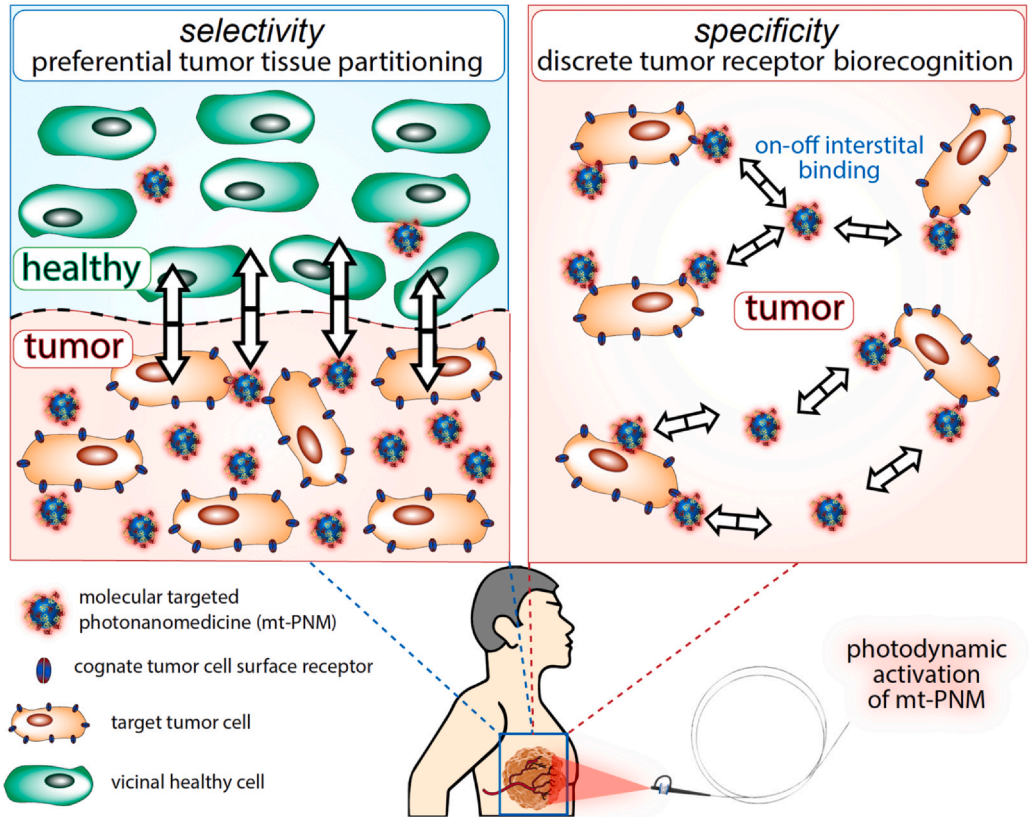

Fig. 1. A conceptual representation of the processes involved in the tumor partitioning of molecular targeted photonanomedicines (mt-PNMs), *i.e.* their selectivity at the μm–mm scale, and mt-PNM biorecognition of cognate tumor cell surface receptors, *i.e.* their specificity which influences their interstitial cellular partitioning at the nm–μm scale.

anatomical locations within those organs [16,17]. Recent findings also allude to the fact that heterogeneity of tumor selective nanoconstruct delivery through the vascular networks is due to inhomogeneity of the fenestrations through which nanoconstructs extravasate into the tumor interstitium, in addition to significant contributions of trans-endothelial transport trough the blood vessels into the tumor interstitium, complicating the mechanics of tumor selectivity further [18].

The conundrum at the nanoscale

The molecular specificity of mt-PNMs is central to their motivation; however, attempting to confer molecular specificity onto nanomedicines can have a drastic and variable impact on tumor selective delivery. This is in part due to the effects that ligand functionalization will have on pharmacokinetics of the nanomedicines, namely the biological nature of the protein corona and the degree of its formation, circulation half-lives, efficiency of bulk tumor selective delivery, tumor retention, and mononuclear cell interactions, amongst several others.

As LTNs generally increase in size within the nanoscale, their pharmacokinetics and *in vivo* tumor selectivity change substantially. Schmidt and Wittrup elegantly modeled the size and affinity-dependence of LTNs on tumor selective delivery [19]. The model predicted that LTNs below 50 nm in diameter exhibited significantly higher tumor selective delivery than their untargeted counterparts; in other words, their molecular specificity directly augments their tumor selectivity. For LTNs greater than 50 nm, their tumor selective delivery is mostly dominated by their size and preferential tumor accumulation, and thus the effect of their specificity, if it even exists, becomes largely unclear. This model has been supported by a number of studies that show that ligand targeting of larger LTNs, such as liposomes and polymeric nanoparticles, has no impact on their tumor selective delivery; however, their specificity has a marked impact on their antitumor efficacy. In one study, Human Epidermal Growth Factor Receptor-2 (HER-2) antibody functionalization of a camptothecin-conjugated polymeric LTN did not improve tumor selective delivery in BT-474 breast tumors, but did result in complete tumor regression, unlike the untargeted constructs [20]. In another study, Epidermal Growth Factor Receptor (EGFR) targeting of liposomal doxorubicin did not increase tumor selective delivery in MDA-MB-468 breast tumors, but did improve the tumor response, compared to an untargeted equivalent [21]. Similar enhanced therapeutic effects of LTN *in vivo* have also been attributed to specificity in the absence of an increase in tumor selective delivery by ligand targeting [22–24]. Even in regards to IgG antibody targeted therapeutics, it has been found that their molecular specificity is predominantly responsible for their antitumor efficacy, while the tumor selective delivery of a non-specific and non-efficacious IgG equivalent was in fact found to be 2.5-fold higher than the targeted IgG antibody [25]. In this instance, the non-specific IgG accumulated 2.5-fold more efficiently within the tumors than the targeted IgG molecule, while remaining unbound. This particular observation is likely a result of the binding site barrier effect which prevents deeper tissue penetration of tumor-specific antibodies as a result of their high avidity towards perivascular tumor tissue [26]. In our report using tumor-activable fluorescent antibody probes for image guided surgery of pancreatic cancer, we show that a non-specific IgG probe exhibits tumor selective properties, as does the targeted cetuximab probe [27]. However, the specificity of the targeted cetuximab probe is only appreciable following spectral unmixing of both probes and subtraction of the non-specific (but selective) accumulation of the sham IgG probe. As such, the tumor selective delivery of LTNs cannot be directly linked to their specificity, nor to their therapeutic efficacy.

Interestingly enough, the notion of tumor selectivity and tumor specificity is well-established in the field of molecular imaging of

solid tumors, especially for *in vivo* diagnostics and image guided surgery [28]. Fluorescent contrast agents, such as methylene blue and indocyanine green are widely adopted in the clinic as tumor-selective probes in the absence of any capacity for molecular recognition. Conversely, molecular targeted fluorescent contrast agents, such as Cetuximab IRDye-800CW conjugates capitalize on tumor tissue EGFR-specific contrast for image guided surgery of head and neck cancer (ClinicalTrials.gov Identifier: NCT03134846), pancreatic cancer (ClinicalTrials.gov Identifier: NCT02736578), esophageal cancer (ClinicalTrials.gov Identifier: NCT04161560) and others. However, it is widely accepted that while probes such as Cetuximab IRDye-800CW detect tumors with high sensitivity, they suffer from sub-optimal specificity (no greater than 69.8%), in part due to their non-specific but tumor-selective accumulation [29]. Of course, non-specific and specific interactions with healthy vicinal tissue also contribute to sub-optimal specificity. For image guided surgery, this lack of clarity due to tumor-selective accumulation has led to the adoption of paired agent imaging as an advanced approach for image guided surgery whereby non-specific but tumor selective accumulation is eliminated in order to improve the accuracy of tumor margin detection [30–32]. In direct contrast, a clear distinction between tumor selective pooling and tumor specific interactions of LTNs and mt-PNMs has not been made to date and in our opinion, has become critical should LTNs and mt-PNMs progress further towards clinical approval.

It is important to emphasize here that for PDT using mt-PNMs, the precise localization of the PS payload molecules at the time of photoactivation dictates their efficacy. This is a direct result of the limited radial diffusion distances of the therapeutic RMS generated in tissue following photoactivation, such as singlet oxygen (70 nm) [33], hydroxyl radicals (8–60 Å) [34,35], hydrogen peroxide (1–10 μm) [36–38], superoxide anion (1 μm) [39], and peroxynitrite radicals (5–20 μm) [40]. Biological radical intermediates are more varied in nature and in their diffusion distances through tissue; however, they still exhibit superior spatial precision in tissue damage than “always-on” cytotoxic or cytostatic agents typically used for conventional LTNs. We have previously shown that intracellularly routing PNMs through specific organelles with submicron precision has a marked impact on efficacy in 2D and 3D tumor models [41,42]. Similarly, we also showed that if a PS payload does not remain tightly associated with its mt-PNM carrier, then the molecular specificity of the construct becomes of little to no value [43]. This appears to be especially problematic for mt-PNMs that consist of a physisorbed or an electrostatically adsorbed PS, as opposed to those chemically conjugated. However, given that an mt-PNM is synthesized with the strongest PS affinity, this spatio-temporal feature of mt-PNMs gives them a distinct advantage over more conventional LTNs in controlling the specificity of tissue damage and confining it to neoplastic tissue. Considering that the majority of emerging NIR activable mt-PNMs integrate multiple therapeutic agents into a single construct, the spatial precision and confinement of the photo-released secondary or tertiary therapeutic payloads will naturally not exhibit the same degree of accuracy of the activated PS that is stably integrated into the mt-PNM. However, considering that photodynamic priming of tumor tissue is a primary motivation for co-encapsulating multiple agents into one therapeutic mt-PNM, they still benefit for molecular targeted photodynamic priming of tumor tissue which exhibits an augmented susceptibility to the secondary or tertiary therapeutic payloads irrespective of their spatial precision when locally released by NIR photodynamic activation.

Aside from the spatial precision of PDT using mt-PNMs, PDT offers an added advantage that can overcome suboptimal tumor selective delivery of nanomedicines, whilst still capitalizing on the advantages of molecular specificity. The effective PDT dose applied to a solid tumor relies on local tumor PS concentrations (a product of the efficiency of tumor selective delivery), oxygen partial pressure and light irradiation parameters [44]. While modulating oxygen partial pressure can be complex, modulating the local tumor PS concentrations depends almost entirely on the efficiency of tumor selective delivery by an mt-PNM system. However; modulating the light dosimetry, in particular the fluence, is an integral part of PDT dosimetry and can in fact even compensate for suboptimal tumor selective delivery that may arise from ligand functionalization of mt-PNMs. It can do so by enabling the customizable deposition of therapeutic RMS doses through the photocatalytic activation of the mt-PNM system. The light fluence can be customized on a tumor-by-tumor basis until a threshold RMS dose is achieved that can impart sufficient tumor tissue photodamage. Light dosimetry itself is complex, but can be monitored implicitly or explicitly through various approaches including imaging of singlet oxygen phosphorescence [45]. This customizable dose deposition of active agents using mt-PNMs is not the case for conventional LTNs, whereby the local dose of a cytotoxic or cytostatic agent delivered to the tumor becomes the only dose available to impart a therapeutic effect. Thus, the dependence on tumor selective delivery by mt-PNMs is theoretically lower than that of LTNs, thereby allowing for the benefits of specificity at the micro-nanoscale within the tumor to be exploited for PDT. This particularly attractive facet of PDT also puts a greater emphasis on the criticality of mt-PNM specificity in order to impart safer, more confined and more efficacious tumor phototoxicity.

In this review, we will discuss the implications of conferring molecular specificity to PNMs and discuss how their specificity and selectivity relate to the efficiency of tumor photodestruction, photodynamic modulation of the mononuclear phagocyte system and vascular system, and the adoption of cutting-edge biomimetic nanotechnologies that augment both mt-PNM specificity and selectivity (Fig. 1).

Distinctive advantages of NIR light activation

PS molecules and some photocatalytic nanoparticles, which serve as both the activating agent and the primary therapeutic agent of mt-PNMs, require activation by a wavelength of light that matches their specific absorption profile. Most PS molecules with clinical potential exhibit multiple absorption peaks spanning the UV–visible-NIR spectrum. The efficiency of RMS photogeneration *in vivo* by a PS is dependent on a high molar extinction coefficient, a high triplet quantum yield, a long triplet state half-life, a high singlet oxygen quantum yield, and a high efficiency of generating radical-based species for the PSs that are capable of doing so [46]. The ideal optical properties of a PS include a high extinction coefficient at an absorption band in the NIR region of the electromagnetic spectrum between 650 nm and 850 nm, which is often referred to as the optical window or the NIR biological window I [47–49]. Visible light typically penetrates tissue from 0.5 mm to 2.5 mm where it exhibits an exponential decrease in intensity as a result of scattering and absorption, with 15–40% of the incident radiation being reflected [50,51]. As such, the appropriate clinical applications of visible light photoactivation for PDT are non-invasive surface malignancies, dermal malignancies and dermal premalignancies [52–55]. Biological tissue exhibits a high extinction coefficient in the UV–visible region (200–650 nm) and IR region (> 2 μm) as a result of absorption by water, melanin, proteins, hemoglobin and deoxyhemoglobin. In addition to the NIR-I biological window, the 1000–1350 nm window (second biological window, NIR-II) and 1500–1800 nm window (third biological window, NIR-III) also exhibits minimized auto-fluorescence, light scattering and light absorption [56,57]. NIR light is therefore generally more effective than visible light when required for use at tissue depths that exceed 0.5 mm [58].

In addition to the depth-dependence of the wavelength of light used to activate mt-PNMs, the penetration depth of NIR light has been found to also depend on the irradiance used [59]. At an irradiance of 1 mW/cm^2 the penetration depth (δ) of 808 nm laser light ($\delta_{808\,nm}$) is 3.4 cm and $\delta_{980\,nm}$ is 2.2 cm; however, at an irradiance of 1000 mW/cm^2, $\delta_{808\,nm}$ increases to 8.4 cm, while $\delta_{980\,nm}$ increases to 5.9 cm [59]. With regards to irradiances, typically non-thermal sub-1 W/cm^2 power densities of NIR light are sufficient for photodynamic activation of mt-PNMs, thereby providing a higher degree of safety and spatial precision in activation and therapy, with respect to photothermally activated nanoconstructs. Additional factors contributing to the effectiveness of NIR photodynamic excitation at various tissue depths include the excitation beam width, energy transfer assistance of PNM nanocarriers, absorption cross section of mt-PNMs, photochemical stability of PS constituents, immunological contribution to deep-tissue tumor damage, and sensitivity of target tissue to RMS species and PDT-based combination regimens [1,50,60–64].

While longer wavelengths are typically more favorable for tissue penetration, PS constituents of mt-PNMs are typically only activated by NIR-I wavelengths of light. This is, in part, due to the limited ability of longer wavelengths (lower energies) to excite PS molecules to energy levels high enough for the generation of singlet oxygen using single-photon excitation processes. This limitation has resulted in the advent of two important advances in PNMs: two-photon NIR photodynamic activation and upconversion-mediated photodynamic activation [65–67]. Two-photon NIR photodynamic activation involves the simultaneous absorption of two NIR photons to excite a higher lying electronic level corresponding to the visible range. The process is inefficient due to intermediate energy levels and requires excitation by an ultra-short pulsed (*e.g.*, femtosecond) laser to provide a high excitation density of ~ 10^6 W/cm^2. As such, although reported *in vivo*, two-photon NIR photodynamic activation of mt-PNMs is challenging in solid tumors. Engineered upconversion nanoparticles (UCNP) can mediate NIR photodynamic activation, whereby UCNPs convert NIR light to visible or UV emission *via* the involvement of real intermediate energy levels in lanthanide ions doped into an appropriate host lattice. The process is significantly more efficient than two-photon NIR photodynamic activation and requires an excitation density of 10^{-1}–10^2 W/cm^2 using a low energy continuous-wave diode laser.

Considering that NIR-I light elicits no tissue toxicity at irradiances sufficient for photodynamic activation, exhibits favorable tissue-penetrating properties, and has a high clinical relevance, it remains to be the wavelength range of choice for the activation of mt-PNMs. The specific role that NIR photodynamic activation plays in the tumor selective and tumor specific properties of mt-PNMs will be discussed further in this review.

Molecular targeted photonanomedicines (mt-PNMs)

The paradox between specificity of binding and specificity of phototoxicity

At the cellular level, molecular specific binding of mt-PNMs is typically achievable *in vitro* using cancer cell-lines; however, cellular specificity of phototoxicity is not always consistent with the patterns of receptor-specific mt-PNM association with cells. The reason for this discrepancy is likely to be a result of the complex interplay between the tumor receptor avidity of the mt-PNMs, the differential rate of cancer cell endocytosis between targeted and untargeted PNMs, the differential rates of mt-PNM endocytosis between cancer and healthy cells, and the differential inherent sensitivities to PDT in cancer and healthy cells, and between the different cancer cells themselves. This phenomenon is likely amplified in cell-line based systems whereby differences inrates of endocytosis between different cell lines can be artificially skewed, and do not provide the natural degree of intracellular variability observed in patient tumor cells. Retrospective analysis of our recently published study using cetuximab targeted photoimmunonanoconjugates (Cet-PINs) reveals that binding specificities in cell lines (*i.e.* extent of receptor-specific mt-PNM association with cells), with respect to untargeted construct, correlated positively with cellular expression levels of EGFR (Fig. 2A) [43]. However, specificity of phototoxicity, depicted as reductions in IC_{50} by molecular targeting, does not correlate with EGFR expression levels in the cell lines tested (Fig. 2B) [43]. For example, the reduction in IC_{50} by molecular targeting of A431 cells was similar to the reduction in IC_{50} by molecular targeting of OVCAR-5 cells, which express an order of magnitude less EGFR per cell than the A431 line. Simply put, the maximum possible enhancement in treatment efficacy was already achieved in OVCAR-5 cells, suggesting an upper level of receptor expression where beyond that, molecular targeting may provide little to no therapeutic enhancements. A study by Peng et al. using a number of cell lines with low-to-moderate EGFR expression found that the specificity of phototoxicity by a cetuximab photoimmunoconjugate (PIC) was not entirely dependent on EGFR expression levels [68]. This therefore suggests that differential cancer cell sensitivities to PDT-induced death pathways is a major contributor to the efficacy of molecular targeted PDT. These findings do not negate the fact that molecular specificity has been proven to enhance the efficacy and safety of PDT, but do underscore the complex processes involved in mt-PNM interactions at the cellular and molecular level, and highlight a significant limitation of cell line-based systems (the most common system used to evaluate mt-PNMs to date) for predicting the specificity of phototoxicity of mt-PNMs. A recent study by Driehuis and

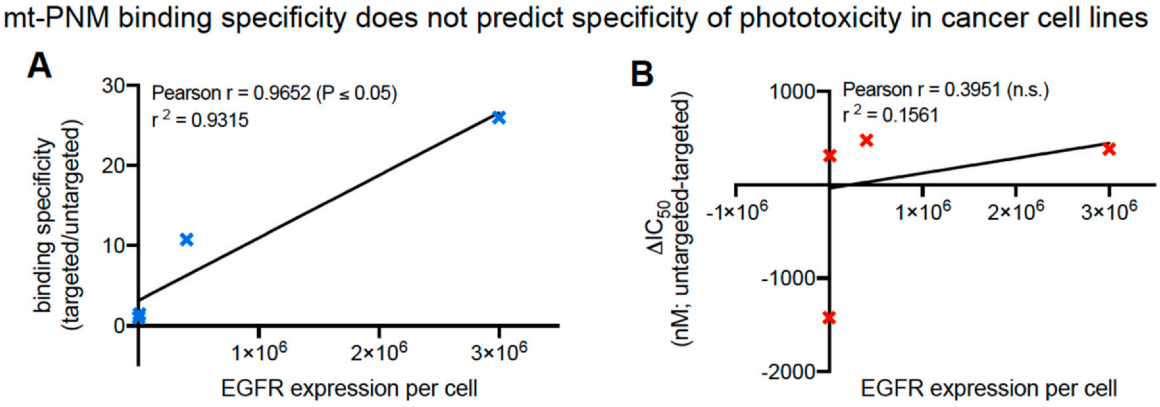

Fig. 2. (A) Binding specificity of the EGFR-targeted mt-PNM (cetuximab photoimmunonanoconjugates; Cet-PIN) correlates positively with cellular EGFR expression levels. (B) The specificity of phototoxicity (difference between IC_{50} of Cet-PIN and untargeted construct) does not correlate with cellular EGFR expression levels, suggesting that molecular targeting is succeeded by complex internalization and phototoxicity events. (Data retrospectively analyzed from our previous study) [43].

Spelier et al. found that the specificity of nanobody-targeted phototoxicity in patient-derived head and neck cancer organoids did in fact significantly correlate with EGFR expression levels [69]. As such, patient-derived tumor organoids are suggested to be better than cell line based *in vitro* models at predicting the efficacy of molecular targeted PDT, as well as recapitulating the target receptor expression levels in the clinic.

Aside from the complex mechanisms of phototoxicity which have been studied in substantial detail in the literature [41,62,70–72], mt-PNM cellular endocytosis parameters in particular need to be taken into consideration when evaluating specificity of phototoxicity both *in vitro* and *in vivo*. The therapeutic benefit provided by the tumor specificity of an mt-PNM system diminishes if the rate of receptor-mediated endocytosis in the cancer cell does not exceed non-specific endocytic routes in the peripheral healthy cells (Fig. 3A) [73–75]. We have previously shown that the fine-tuning of surface ligand density on mt-PNMs expedites endocytosis in cancer cells in addition to optimizing their binding specificity [43]. The relationship between nanoconstruct size and ligand density has been modeled elegantly by Zhang et al. (Fig. 3B), who suggested that small constructs with higher surface densities will exhibit faster rates of receptor-mediated endocytosis. Such models help serve as a guide to design multifaceted mt-PNM systems with the greatest degree of specificity in phototoxicity [76]. In addition, fine tuning mt-PMN parameters such as construct size, charge, morphology, surface area and aspect ratio is also critical for conferring specificity of phototoxicity [73,76]. How the interdependence of these parameters affects the specificity of phototoxicity *in vivo* is yet to be investigated in detail, and likely requires the use of heterogeneous patient-derived tumor models that recapitulate the degree of tumor receptor overexpression and the heterogeneity in overexpression, endocytic rates and PDT sensitivities observed in patients. What these models do provide however, is further insights into the mt-PNM-specific parameters leading to the paradox between specificity of binding and specificity of phototoxicity. The radius of mt-PNMs and ligand density on the surface of mt-PNMs directly affect the sterics of target receptor engagement on cancer cell membranes. Furthermore, the receptor expression levels on the cancer cell membranes provide an additional, yet simultaneous, variable on the sterics of target receptor engagement by mt-PNMs. Ultimately what these multi-parametric variables result in is a non-linearity in the system whereby steric hindrance of mt-PNM recognition and inhomogeneous receptor clustering can exert drastic limitations on the triggering of cancer-cell specific internalization. In that case, the rate of internalization on an untargeted PNM may become equal to the rate of internalization of cancer cell bound mt-PNMs, thereby providing no real advantage of molecular targeting. In addition, certain ligands used for mt-PNM functionalization can quench therapeutic RMS species, and thus although mt-PNMs may exhibit tumor cell-specific binding, the anticipated enhancement in therapeutic efficacy provided by targeting is diminished to a certain degree by RMS quenching [77]. Together, these discrepancies, added to the intrinsic inter-cellular variability of PDT-responsiveness, complicate mt-PNM systems considerably and contribute to the paradox that we discuss.

In light of this paradox between mt-PNM binding specificity and specificity of phototoxicity, it becomes apparent that, although wide-spread, cell line-based *in vitro* and *in vivo* tumor models are not ideal for evaluating the therapeutic contribution of mt-PNM specificity. Using a single cell line transfected with tumor receptors can prove to be helpful in evaluating mt-PNM specificity of phototoxicity, however certain receptors, such as growth factor receptors, may cause the transfected cells to exhibit expedited growth rates and dampened treatment responses. Patient-derived 3D tumor nodules and organoids can provide a powerful and high throughput platform for the screening of mt-PNM therapeutic efficacy. They recapitulate patient cellular and molecular heterogeneity and provide an option for low-receptor-expressing healthy tissue organoids as negative controls. In the case of *in vivo* PDX models, while they might be more informative than single-cell line tumor models as they also naturally recapitulate patient cellular and molecular heterogeneity, negative controls for low receptor expression may be difficult to obtain and the treatment results are equally difficult to interpret without performing high-volume experiments using a panel of PDX tumors. Syngeneic tumor models could also prove to be valuable in that regard, but often suffer from limited cross-species reactivity with targeting ligands that are primarily directed towards human receptors. Thus, it appears that utilizing multiple tumor models simultaneously can be the most reliable method to evaluate mt-PNM specificity of phototoxicity *in vivo* prior to clinical trials.

Tumor selective delivery: fundamental concepts and motivation

For the majority of pre-clinical anti-cancer nanomedicines under development, one of the primary motivations for leveraging nanoparticle drug delivery systems is to promote bulk tumor selective delivery of the therapeutic agents by extending their circulation half-lives. For hydrophobic PSs specifically, which constitute a significant proportion of all clinical and pre-clinical PSs, an additional motivation for nanoformulation is to preserve their monomeric non-aggregated state within the body, and thus preserve their PDT activity. While this is not the case for a small proportion of PSs that exhibit aggregation-induced emission characteristics, this is certainly one of the

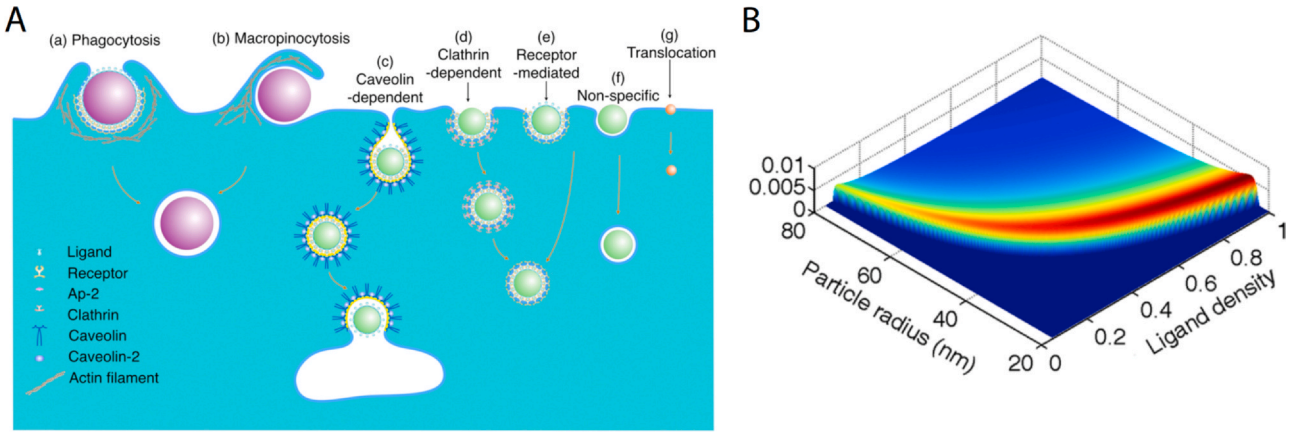

Fig. 3. (A) Nanoconstruct endocytic pathways in cells including those involved in non-receptor mediated (a, b) and receptor mediated (c–e) processes. (B) Modeling to predict the relationship between the nanoconstruct size and ligand density on cellular endocytosis rate.
Reprinted and adapted with permission from [76]. Copyright (2015) American Chemical Society.

predominant motivations for the use of PNMs such as Visudyne® (nanoliposomal benzoporphyrin derivative), FosLip® (nanoliposomal 5,10,15,20-Tetrakis(3-hydroxyphenyl)chlorin; mTHPC) and FosPEG® (PEG modified nanoliposomal mTHPC). Nanoformulation of PSs and other small molecular anticancer agents typically modifies their pharmacokinetic profile and modulates their clearance pathways in order to promote accumulation within the tumor. Although these processes that contribute to the tumor selectivity of PNMs are attributed to the EPR effect, the EPR effect in of itself is emerging to be a complex combination of nanoconstruct size-dependent processes that involve passive permeation through vascular fenestrations, active transcytosis through the vascular endothelium and compromises in lymphatic drainage [16–18].

While this review attempts to provide a clear demarcation between the processes underlying mt-PNM specificity and selectivity, the processes underlying tumor selectivity are analogous with those by which nanoconstructs are delivered to tumors. Thus, the degree of tumor selectivity of a nanoconstruct is contingent on the efficiency of its delivery to tumors, yet the notion of tumor preference is unique to the definition of tumor selectivity. It is important to emphasize that specific qualification, as some strategies which improve the efficiency of nanoconstruct tumor delivery will also promote normal tissue accumulation, thereby not providing a greater degree of tumor selectivity. A literal distinction between tumor selectivity and tumor delivery is also important as the metrics used in the literature to report delivery (*e.g.* % injected dose) are different from those used to report selectivity (*e.g.* tumor-to-normal ratio), even though the latter is contingent on the former. In this review, we refer to tumor selective delivery as the process by which tumor delivery is enhanced with respect to healthy tissue. In an elegant report by Wilhelm et al., a thorough meta-analysis of the literature has been presented with regards to how tumor delivery and selectivity of a plethora of nanoconstructs have evolved over the past decade [78]. The various strategies used to modulate tumor delivery and tumor selective delivery are exhaustively discussed and their true effectiveness has been evaluated. A more recent 15-year meta-analysis study by Cheng et al. exploring nanoconstruct tumor delivery used physiologically based pharmacokinetic modeling and simulation to predict the behavior of nanoconstruct delivery in tumors, taking various physiological parameters into consideration (*eg.* plasma, organ retention, clearance routes *etc.*) [79]. The study found that tumor selective delivery was largely limited by low distribution and permeability coefficients at the tumor site, both of which have been shown to be augmented by NIR-PDT [80–83]. The meta-analysis by Cheng et al. also found that only the mean tumor delivery (not the median tumor delivery) was enhanced by ligand targeting of nanoconstructs, which was also consistent with the findings of the meta-analysis by Wilhelm et al. [78,79] The significance of this finding is that it suggests that tumor tissue specificity does influence tumor selective delivery to a certain degree; however, determining to what extent the nanoconstruct present in a tumor is exhibiting selectivity verses specificity remains to be largely abstract.

Our recent study attempted to distinguish between tumor specificity and selectivity by leveraging quantitative NIR molecular imaging to measure the tumor specificity of an NIR-active EGFR-targeted LTN *in vivo* [84]. By using a binding potential model based on paired agent imaging the concentration of *in vivo* tumor EGFR was calculated. This tumor EGFR concentration reported by the EGFR-targeted LTN was consistent with pre-determined EGFR concentrations in the same tumor type, thereby providing a quantitative metric for how much specificity the LTN exhibited for its target receptor *in vivo.* Importantly, this LTN's specificity for *in vivo* EGFR correlated linearly with the EGFR expression of the tumor *ex vivo* and *in vitro.* However, this correlation was not observed between EGFR expression and tumor selectivity (tumor-to-healthy brain ratio) or between EGFR expression and tumor delivery (%I.D./g). While this non-invasive quantitation of LTN specificity was demonstrated in a nanoliposomal system, the approach is in theory amenable to any LTN targeted to any receptor or non-receptor target. Although this approach provides a means to quantify LTN specificity, it is apparent from the literature that delineating the therapeutic contributions of mt-PNM specificity and selectivity remains to be a significant challenge, which is critical for justifying and motivating molecular targeting.

Delineating the therapeutic contributions of specificity from selectivity

A plethora of elegant, insightful and detailed studies have been described for cutting-edge mt-PNMs. The overall increase in tumor selective delivery provided by formulating small molecule PSs in these mt-PNMs has oftentimes shown striking improvements in antitumor PDT efficacy. However, a number of these studies have further attempted to probe and delineate the contribution of molecular specificity, as provided by ligand functionalization, in the improved therapeutic outcomes observed. These strategies, however, have their own respective limitations that can further skew the interpretation of what the real therapeutic contributions of molecular specificity may be. For example, a receptor-null tumor line proposed as a negative control may exhibit distinctly different genetic, epigenetic and phenotypic profiles than the experimental tumor, thereby exhibiting inherently different responses to PDT irrespective of the degree of molecular recognition. Likewise, ligand-free control nanoconstructs are likely to exhibit markedly different circulation half-lives, clearance mechanisms and tumor tissue partitioning than the mt-PNM's. These approaches, and others are discussed in greater detail in this section. The therapeutic contribution of mt-PNM specificity in the key studies discussed in this section are summarized in Table 1. Table 2 provides a summary of the advantages, disadvantages and clinical status of common targeting ligands used for mt-PNMs. While this section provides a detailed summary of the strategies for ligand decoration of mt-PNMs and the NIR photodynamic activation approaches for target-specific photoactivation and destruction, the criticality of demarking the implications of tumor specificity and tumor selectivity remain to be the emphasis of this review article.

Specificity using antibody formats and antigen recognition molecules

The majority of targeted therapeutics and targeted imaging agents used in clinical studies and clinical practice are all based on antibody conjugates. In addition, the majority of LTNs in clinical trials are based on antibody format functionalized nanomedicines. As such, antibodies, antibody fragments, formats, and engineered antigen recognition molecules are of high clinical relevance for fabricating mt-PNMs.

In our recent study, we used an EGFR antibody (cetuximab)-targeted liposomal formulation of benzoporphyrin derivative (Cet-PIN) as a platform to tune multiple interdependent nanoconstruct variables in order to impart the greatest degree of molecular specificity in PDT of desmoplastic pancreatic adenocarcinoma [43]. These variables include the orientation and surface density of conjugated cetuximab, the Cet-PIN electrostatic charge, and the membrane anchoring of benzoporphyrin derivative using multiple lipid conjugates (Fig. 4A). The tuned Cet-PINs exhibited up to 100-fold binding specificity in 2D cells *in vitro.* Up to 16-fold specificity in phototoxicity was observed in 3D heterotypic tumor nodules comprising of MIAPaCa-2 ($EGFR^+$) pancreatic cancer cells and patient-derived cancer-associated fibroblasts (PCAFs; $EGFR^+$), as compared to untargeted constructs. Nodule destruction was promoted further by Cet-PIN loading with oxaliplatin, gemcitabine and 5-fluorouracil. As *in vivo* molecular specificity of phototoxicity was the ultimate goal, the PDT efficacy of the Cet-PINs was evaluated in desmoplastic MIA PaCa-2 + PCAF tumors. 72 h following PDT, significant necrosis was

Table 1
A summary of key mt-PNM studies that explore ligand targeting for PDT-based treatment of solid tumors. Findings that delineate the therapeutic contribution of specificity, if any, are highlighted for each study.

mt-PNM core construct	Photosensitizer	Ligand	target	mt-PNM diameter	mt-PNM dosing	Photodynamic activation parameters[a]	Therapeutic contribution of mt-PNM specificity
nanoliposomes	lipid-anchored benzoporphyrin derivative	cetuximab	EGFR	134.7 nm	0.5 mg/kg	690 nm 150 J/cm^2 100 mW/cm^2 12 h P.L.I.	specificity results in a 3-fold enhancement in tumor photodestruction, mitigation of local and systemic phototoxicity; non-specific PNM controls alone exert minimal phototoxic anti-tumor effects [43]
polymeric micelles	Meta-tetra (hydroxyphenyl) chlorin	EGa1 nanobody	EGFR	17 nm 24 nm 45 nm	0.3 mg/kg	N/A	micelles retained prolonged circulation times following ligand conjugation promoting tumor selective delivery; future therapeutic studies are warranted to delineate differences between tumor specific and tumor selective phototoxicity [85]
cera nanoparticles	chlorin e6	folic acid	folate receptor	3–5 nm	20 μM PS equivalent in 100 μL	660 nm 18 J/cm^2 100 mW/cm^2 4 h P.L.I	specificity results in a 2-fold enhancement in tumor growth inhibition, as compared to tumor selective tumor growth inhibition by a non-specific PNM control [86]
upconversion nanoparticles	zinc(II) phthalocyanine	folic acid	folate receptor	50 nm	2.88 mg/kg	660 nm; 980 nm 360 J/cm^2 200 mW/cm^2 24 h P.L.I	ligand targeting enhances tumor-to-skin selectivity of nanoparticles by 2-fold; phototoxicity as a result of tumor selectivity or tumor specificity has not been explored [87]
PLGA (polylactic-co-glycolic acid) nanoparticles	pheophorbide a	folic acid	folate receptor	100–150 nm	N/A	N/A	contribution of specificity to tumor selective delivery *in vivo* unclear; phototoxicity as a result of tumor selectivity or tumor specificity has not been explored [88]
carbon nanodots	zinc(II) phthalocyanine	folic acid	folate receptor	2–8 nm	0.5 mg/kg	660 nm 120 J/cm^2 300 mW/cm^2 12 h P.L.I	specificity is entirely responsible for all tumor photodestruction; tumor selective but non-specific PNM controls exert no phototoxic anti-tumor effects [89]
nanoliposomes	Bis-Pyrene or MC4	folic acid	folate receptor	N/A	200 μL PS at 4 mg/ml	808 nm 2,100 J/cm^2 4,400 mW/cm^2	tumor growth inhibition likely a result of combined tumor selective and tumor-specific processes; the contribution of specificity for phototoxicity *in vivo* is undetermined [90]
porphysomes	pyropheophorbide-lipid conjugate	folic acid	folate receptor	130 nm	10 mg/kg	671 nm 100 J/cm^2 150 mW/cm^2	targeting reduces tumor selectivity by 2-fold; specificity enhances tumor control by 7-fold and extends survival [91]
titanium dioxide nanoparticles	titanium dioxide nanoparticles and titanocene	transferrin	transferrin receptor	108 nm	1 mg/kg	N/A	targeting increases selectivity by 7-fold; tumor growth inhibition likely a result of combined tumor selective and tumor-specific processes; the contribution of specificity for phototoxicity *in vivo* is undetermined [24]
nanoliposomes	aluminum phthalocyanine tetrasulfonate	transferrin	transferrin receptor	146 nm	400 μM of mt-PNM	N/A	specificity is responsible for all tumor selective accumulation; no phototherapeutic efficacy was observed *in vivo* [92]
gold nanoparticles	silicon phthalocyanine	prostate specific membrane antigen ligand (PSMA -1)	prostate specific membrane antigen	27 nm	0.07 mg/kg	672 nm 150 J/cm^2 or 300 J/cm^2 100 mW/cm^2 3 h P.L.I	specificity enhances selectivity in receptor-positive tumors by 4-fold, therapeutic contribution of specificity *in vivo* is undetermined [93]
iron oxide nanoparticles	silicon phthalocyanine	fibronectin mimetic protein	Integrin β1 receptor	10 nm	0.06 mg/kg 0.4 mg/kg	672 nm 150 J/cm^2 100 mW/cm^2 48 h P.L.I	specificity enhances tumor selective delivery by 20% and phototherapeutic efficacy by 2-fold; enhanced phototherapeutic efficacy only observed when using a low (0.06 mg/kg) administered dose of nanoparticles [94]
nanographene	HPPH	HK peptide	Integrin αvβ6 receptor	10-100 nm	30 nmol PS equivalent	671 nm 70 J/cm^2 10 mW/cm^2 24 h P.L.I	specificity enhances selectivity by 1.57-fold, true phototherapeutic contribution of specificity *in vivo* is undetermined [95]

(*continued on next page*)

Table 1 (*continued*)

mt-PNM core construct	Photosensitizer	Ligand	target	mt-PNM diameter	mt-PNM dosing	Photodynamic activation parameters[a]	Therapeutic contribution of mt-PNM specificity
hyaluronic acid nanoparticles	chlorin e6	hyaluronic acid nanoparticle framework	CD44	227 nm	5 mg/kg	671 nm 180 J/cm^2 100 mW/cm^2 24 h P.L.I	phototherapeutic efficacy likely a result of combined tumor selective and tumor-specific processes; the therapeutic contribution of specificity *in vivo* is undetermined [96]
hexa-decapeptide nanoparticles	indocyanine green derivative	hyaluronic acid folic acid	CD44 folate receptor	24 nm	5 mg/kg	808 nm 60 J/cm^2 1,000 mW/cm^2 24 h P.L.I	specificity enhances selectivity by 3-fold, promoted tumor growth inhibition by 2-fold and increases cure rates by 5-fold [97]
super paramagnetic nanoparticles	chlorin e6	folic acid	folate receptor	7 nm	5 mg/kg PS equivalent	633 nm 90 J/cm^2 50 mW/cm^2 30 min P.L.I	phototherapeutic efficacy likely a result of combined tumor selective and tumor-specific processes; therapeutic contribution of specificity *in vivo* is undetermined due to absence of non-specific PNM controls [98]
Zr-based nanoscale Metal Organic Framework	TMPyP4	G4-sgc8 aptamer	protein tyrosine kinase 7	93 nm	50 μL of 2 mg/mL mt-PNM equivalent	660 nm 3600 J/cm2 2 W/cm^2 2 h P.L.I	specificity is entirely responsible for all tumor photodestruction; tumor selective but non-specific sham aptamer-functionalized PNM controls exert no phototoxic anti-tumor effects, intratumoral administration confounds interpretation of drug delivery [99]

[a] P.L.I. refers to PS-light interval.

observed and quantified from the H&E stains only in the tumors treated with the targeted Cet-PINs (Fig. 4B). In order to substantiate the observation that true specificity in phototoxicity was achieved *in vivo,* we evaluated the PDT efficacy of the Cet-PINs in the low EGFR-expressing T47D tumors, and showed that no necrosis was induced (Fig. 4C). Interestingly, although the untargeted constructs exhibited no anti-tumor efficacy, they resulted in blistering and necrosis of the nearby tissues, bowel perforation and signs of severe toxicity and moribundity 72 h after PDT (Fig. 4D, E). While our findings strongly suggest that molecular specificity is responsible for the pronounced anti-tumor effect and negligible healthy tissue destruction, they also suggest that the healthy tissue clearance of the untargeted construct may be slower than that of the Cet-PINs. If this were the case, it would likely be a result of the surface-bound antibody which promotes macrophage clearance. To substantiate this hypothesis, full pharmacokinetic and pharmacodynamic studies are warranted. The role of macrophages in PDT using mt-PNMs will also be discussed further in section *The mt-PNM – mononuclear phagocyte system (MPS) axis*.

In a recent detailed study by Liu et al., the impact of nanobody molecular targeting of polymeric micelles on their *in vitro* specificity and pharmacokinetics has been investigated [85]. Motivated by the concept that smaller nanoconstructs exhibit favorable tumor tissue penetration profiles, the authors prepared polymeric micelles based on benzyl-poly(ε-caprolactone)-b-poly (ethylene glycol) of three different diameters 17 nm, 24 nm and 45 nm encapsulating the PS Meta-tetra(hydroxyphenyl)chlorin (mTHPC). The untargeted micelles were compared to micelles further functionalized with an EGFR targeting nanobody, EGa1. The photocytotoxicity of EGa1-P23 micelles loaded with mTHPC was 4-fold higher in EGFR over-expressing A431 cells than the untargeted micelles (Fig. 5A), and demonstrated preferential phototoxicity towards A431 cells over low-EGFR expressing HeLa cells. It was found that both the plasma half-lives and the Area Under the Curve (AUC) of the nanobody targeted micelles was largely unaltered in A431 tumor bearing-mice, as compared to untargeted micelles (Fig. 5B). These findings are of significant importance as they identify a discrete set of parameters for fabricating micelle-based mt-PNMs without compromising their pharmacokinetic properties, thereby further maximizing their potential therapeutic benefit.

Specificity using small molecular weight ligands

Owing to its biocompatibility, small molecular weight, chemical stability and facile conjugation, folic acid (FA) is one of the most heavily explored small molecular weight ligands for mt-PNMs used to confer specificity for the widely expressed tumor-associated folate receptor (FR).

In a study by Li et al. cerium oxide (cera) nanoparticles (3–5 nm diameter) coated with polyethylenimine-PEG (PPCNP) were prepared [86]. The PPCNP nanoparticles were modified with chlorin e6 (Ce6) as the PS and with FA to target FR overexpressed on Adriamycin resistant human breast cancer cells (MCF-7/ADR). *In vitro*, molecular targeting resulted in a mild 1.2-fold greater cell fluorescence intensity of the PPCNPs-Ce6/FA than the untargeted PPCNPs-Ce6 nanoparticles. However, the effects of molecular targeting on nanoparticle tumor selective delivery and photodestruction were more pronounced *in vivo*. A higher fluorescence intensity was observed in MCF/ADR tumors following administration with the targeted PPCNPs-Ce6/FA nanoparticles, as compared to untargeted PPCNPs-Ce6 and free Ce6 (Fig. 6A). The tumor growth inhibition by PDT of the targeted PPCNPs-Ce6/FA was *ca.* 2-fold more effective than untargeted PPCNPs-Ce6 controls (Fig. 6B), a difference which can be almost entirely attributed to specificity. Mice treated with PPCNPs-Ce6/FA showed a 96% reduction in tumor volume but with untargeted PPCNPs-Ce6 the reduction was only 52%, which can be attributed to tumor selective uptake. Moreover, the tumors from

Table 2
A summary of the advantages and disadvantages of targeting ligands commonly used for mt-PNMs in addition to their clinical status as therapeutics, tumor contrast agents or LTN targeting moieties.

Targeting ligands	Advantages	Disadvantages	Clinical use of ligand for LTNs (ClinicalTrials.gov identifier[a])	Example of other clinical use of ligand (ClinicalTrials.gov identifier*)
full-length antibodies	• high sensitivity • high diversity of potential targets • long circulation half-lives • highly reproducible and scalable	• clearance by FcγR+ leukocytes when conjugated to LTNs • immunogenicity • large molecular weight impacts overall size of LTN • moderate-to-low physical and chemical stability • issues with specificity • moderate tumor penetration • nanoconjugation can impair avidity	• **TargomiRs**: anti-EGFR bispecific antibody targeted minicells encapsulating miR-16-based microRNA mimic (NCT02369198)	• functional blocking (NCT04375384) • antibody-dependent cell cytotoxicity (NCT02954536) • antibody-drug conjugates (NCT03530696) • image guided surgery (NCT03134846) • immunotherapy (NCT04212026) • photoimmunotherapy (NCT04305795)
antibody fragments	• high sensitivity and specificity • no clearance by FcγR+ leukocytes when conjugated to LTNs thereby minimizing effect on pharmacokinetics • high tumor penetration • high diversity of potential targets • long circulation half-lives	• moderate-to-low physical and chemical stability • nanoconjugation can impair avidity	• **SGT-53**: anti-transferrin scFv targeted liposome encapsulating p53 gene (NCT02340117) • **anti-EGFR-IL-dox**: EGFR scFv targeted liposome encapsulating doxorubicin (NCT02833766) • **SGT-94**: transferrin receptor scFv targeted liposome encapsulating RB94 gene (NCT01517464)	• clot prevention (NCT00420030) • macular degeneration (NCT04332133) • Chron's disease (NCT03357471)
nanobodies	• high sensitivity and specificity • high tumor penetration • rapid tumor binding and clearance of non-specific accumulation • Little to no immunogenicity • high diversity of potential targets • high physical and chemical stability • short circulation half-lives • small molecular weight has minimal impact on overall size and pharmacokinetics of LTN • conjugation to LTN has minimal impact on circulation half-lives	• short circulation half-lives • nanoconjugation can impair avidity	N/A	• immunotherapy (NCT04503980) • clot prevention (NCT01151423) • psoriasis (NCT03384745) • CAR-T cell immunotherapy (NCT03758417)
folic acid	• no immunogenicity • small molecular weight has minimal impact on overall size and pharmacokinetics of LTN • short circulation half-lives • well-defined binding process • high prevalence of expression of *in vivo* molecular target • site-specific conjugation guarantees target engagement		N/A	• image guided surgery (NCT03180307) • folate-drug conjugates (NCT01170650)
transferrin	• well-defined binding process • high prevalence of expression of *in vivo* molecular target	• immunogenicity • intermediate molecular weight impacts overall size of LTN • moderate-to-low physical and chemical stability • nanoconjugation can impair avidity	• **MBP-426**: transferrin-targeted liposome encapsulating oxaliplatin (NCT00964080)	• atransferrinemia (NCT01797055)
synthetic peptides	• small molecular weight has minimal impact on overall size and pharmacokinetics of LTN • strong binding affinity • high diversity of potential targets • short circulation half-lives • site-specific conjugation guarantees target engagement	• prone to aggregation • short circulation half-lives	• **REXIN-G**: peptide-functionalized retroviral expression vector encapsulating cyclin G1 gene (NCT00572130) • **BIND-014 (terminated)**: PSMA-1 targeted polymeric nanoparticle encapsulating docetaxel (NCT02479178)	• nanoconjugate for image-guided intraoperative mapping of nodal metastases (NCT02106598) • image guided surgery (NCT03470259)

(*continued on next page*)

Table 2 (*continued*)

Targeting ligands	Advantages	Disadvantages	Clinical use of ligand for LTNs (ClinicalTrials.gov identifier[a])	Example of other clinical use of ligand (ClinicalTrials.gov identifier[a])
aptamers	• small molecular weight has minimal impact on overall size and pharmacokinetics of LTN • high diversity of potential targets • short circulation half-lives • site-specific conjugation guarantees target engagement	• susceptibility to enzymatic degradation • short circulation half-lives • rapid renal clearance • risk of target cross-reactivity	N/A	• colorimetric sensors for cancer staging (NCT02957370) • macular degeneration (NCT01089517)

[a] Example of relevant ClinicalTrials.gov identifier, Accessed October 2020.

mice treated with PPCNPs-Ce6/FA were found to have large areas of necrosis and damaged blood vessels. Prior evaluation of lung and pancreatic cancer patient tissue found FR expression in more than 80% of peritumoral healthy cells including endothelial cells [100]. It is thus likely that FR-targeted mt-PNMs can also induce molecular-specific photodamage to tumor vasculature. While the circulation half-life of these nanoparticles is unknown, it is not possible to speculate on the nanoparticle content remaining in the tumor blood vessels at the time of irradiation (24 h after administration). However, these findings are consistent with previous work which shows that a combination of cellular photodamage and vascular photodamage is most effective [101,102]. Thus, PDT strategies that intelligently combine vascular photodamage in addition to molecular targeted photodamage to receptor-overexpressing tumor cells may in fact prove to be most efficacious. It can also be speculated that the smaller size of these ceria nanoparticles contributed to the effectiveness of tumor selective delivery in response to FA targeting, which is not as pronounced *in vivo* in the other studies described here.

While the majority of mt-PNM studies have focused on using nanoconstructs as high-payload PS carriers, and platforms for ligand functionalization, other studies have leveraged the inherent photophysical properties of the nanoconstruct itself. A study by Cui et al. used oleic acid upconversion nanoparticles (OA-UCNP) as platforms for deep-tissue molecular targeted PDT [87]. The (OA-UCNP) were functionalized with the PS zinc(II) phthalocyanine (ZnPc) and were coated with FA-modified chitosan (FASOC) to confer molecular specificity for FR; the whole nanoconstruct had a diameter of *ca.* 50 nm. FR negative A549 cells exhibited low uptake of the targeted OA-UCNP nanoparticles, with higher uptake observed in Bel-7402 and MDAMB-231 FR-positive cells. Imaging-based biodistribution studies demonstrated that targeted OA-UCNP nanoconstruct accumulation was higher in Bel-7402 tumors than untargeted nanoconstructs (Fig. 7A). The tumor-to-skin ratio of selectivity for the targeted construct was found to be *ca.* 12 at 24 h, whereas the highest tumor-to-skin ratio of selectivity for the untargeted construct was *ca.* 5 at 24 h (Fig. 7B). The data confirmed that for this particular mt-PNM system, its specificity for FR directly improved its tumor selective delivery. Evaluation of the PDT efficacy was also performed in mice implanted with S180 murine sarcoma tumors and Bel-7402 tumors. The mice were irradiated with either 660 nm for direct PS excitation or with 980 nm for indirect upconversion-mediated PS excitation. While for subcutaneous tumors 660 nm laser irradiation was found to be effective, for deeper tumors (1 cm deep) irradiation with 980 nm light was more effective (Fig. 7C). While this study showed that the specificity of the UCNP nanoconstructs increases tumor selectivity significantly, it remains unclear to what extent specificity contributes to the substantial PDT tumor responses observed.

In addition to the inorganic nanoparticles discussed, organic and biodegradable mt-PNMs have been engineered to elicit FA-mediated tumor specific photodamage. In a study by Son et al. PLGA nanoparticles (100–150 nm diameter) containing the PS pheophorbide (Pba) were modified with PEG and FA to confer PDT specificity to FR (Fig. 8A) [88]. *In vitro*, the targeted FA-PLGA-Pba construct exhibited higher cellular accumulation and only marginal enhancements in cell death in FR-over-expressing MKN28 cells compared to the untargeted construct. These findings are somewhat consistent also with prior *in vitro* studies which showed that FA targeting of liposomal mTHPc and zinc tetraphenylporphyrin enhances the photodynamic efficacy by two fold [103,104]. Although both MKN28 tumor selectivity and bulk tumor delivery of the FA-PLGA-Pba construct was improved 10-fold, as compared to the free Pba PS, it is unclear what the role of specificity is in the tumor selective delivery of this mt-PNM (Fig. 8B). PDT efficacy was also not explored in this study, and while FA targeting of this mt-PNM appears to be somewhat promising, the contribution of molecular specificity for targeted photodamage is yet to be explored.

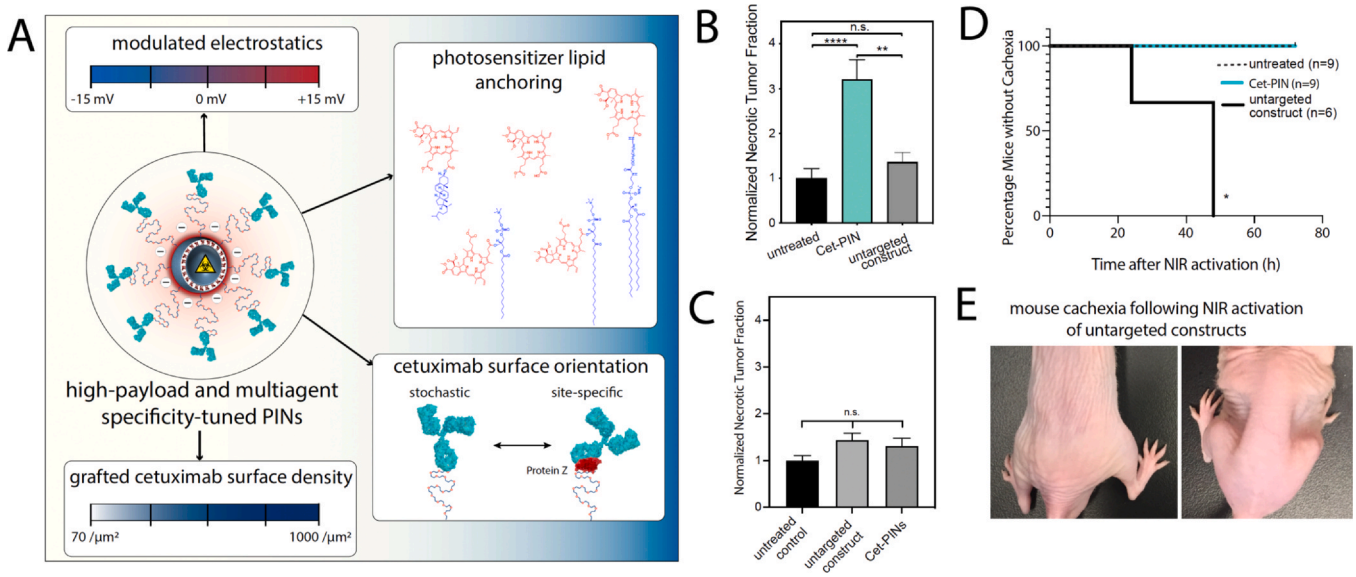

Fig. 4. (A) Schematic diagram representing the specificity tuning of the photoimmunonanoconjugates (PINs). (B) Photodynamic activation of Cet-PINs showed a significant increase in tumor necrosis, as compared to tumors treated with tumors untargeted constructs. (C) No significant difference in necrosis shown between targeted and untargeted constructs was observed in low-EGFR expressing T47D tumors. (D) Incidence of acute mouse cachexia 72 h following PDT treatment. Cachexia was observed in 100% of mice treated with untargeted constructs (E) whereas mice in the untreated group and the targeted treatment group remained healthy. (E) Representative photograph of mouse cachexia 72 h following PDT of untargeted constructs administered to mice bearing MIA PaCa-2 + PCAF heterotypic tumors (right), as compared to untreated mice (left).
Adapted with permission from [43]. Copyright (2019) American Chemical Society.

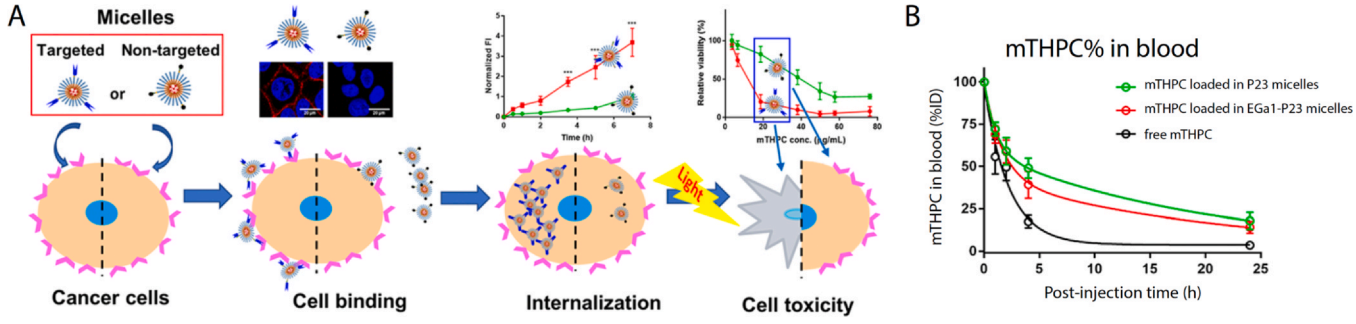

Fig. 5. (A) Schematic diagram showing the difference between untargeted and molecular targeted *in vitro* PDT with mTHPC PS loaded micelles, exemplifying their specificity in binding, uptake and phototoxicity. (B) Blood circulation profiles of free mTHPC, untargeted mTHPC-loaded micelles and nanobody-targeted mTHPC micelles after intravenous administration in A431 tumor bearing mice. Ligand targeting did not significantly compromise the favorable pharmacokinetic profiles of the micelles.
Reproduced with permission from https://pubs.acs.org/doi/10.1021/acs.molpharmaceut.9b01280 [85]. Further permissions related to the material excerpted should be directed to the ACS.

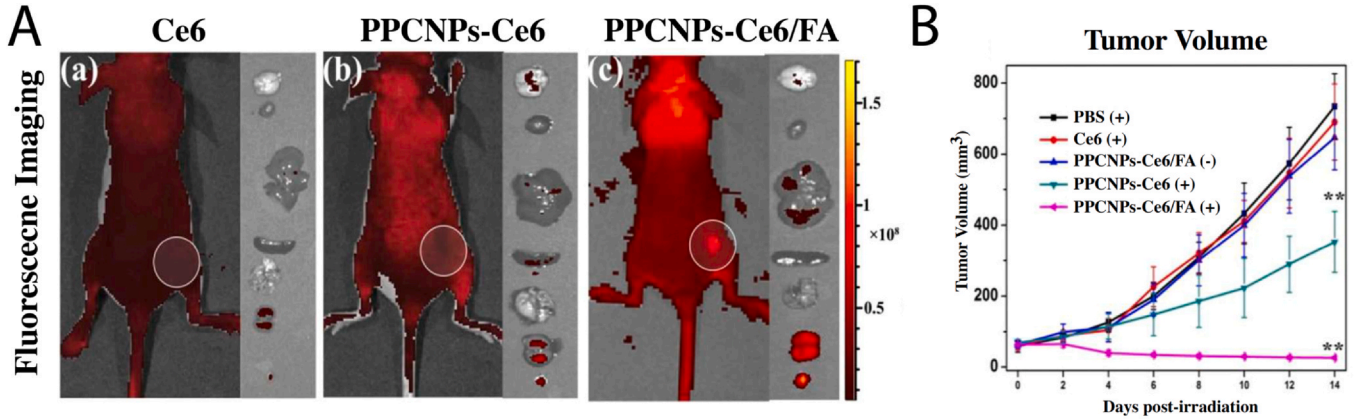

Fig. 6. (A) NIR fluorescence imaging of mice carrying the drug resistant MCF-7/ADR human tumors 24 h after intravenous injection of Ce6 (PS), PPCNPs-Ce6 (untargeted nanoparticles and PS) and PPCNPs-Ce6/FA (nanoparticles conjugated with PS and targeting ligand). Higher accumulation in tumor tissue was observed in the group with FR targeting. (B) Tumor growth curves for MCF-7/ADR tumor bearing mice treated in five different groups. The most significant decrease in tumor volume is observed in the mice treated with the targeted PPCNPs-Ce6/FA nanoconstruct.
Adapted with permission from [86]. Copyright (2016) American Chemical Society.

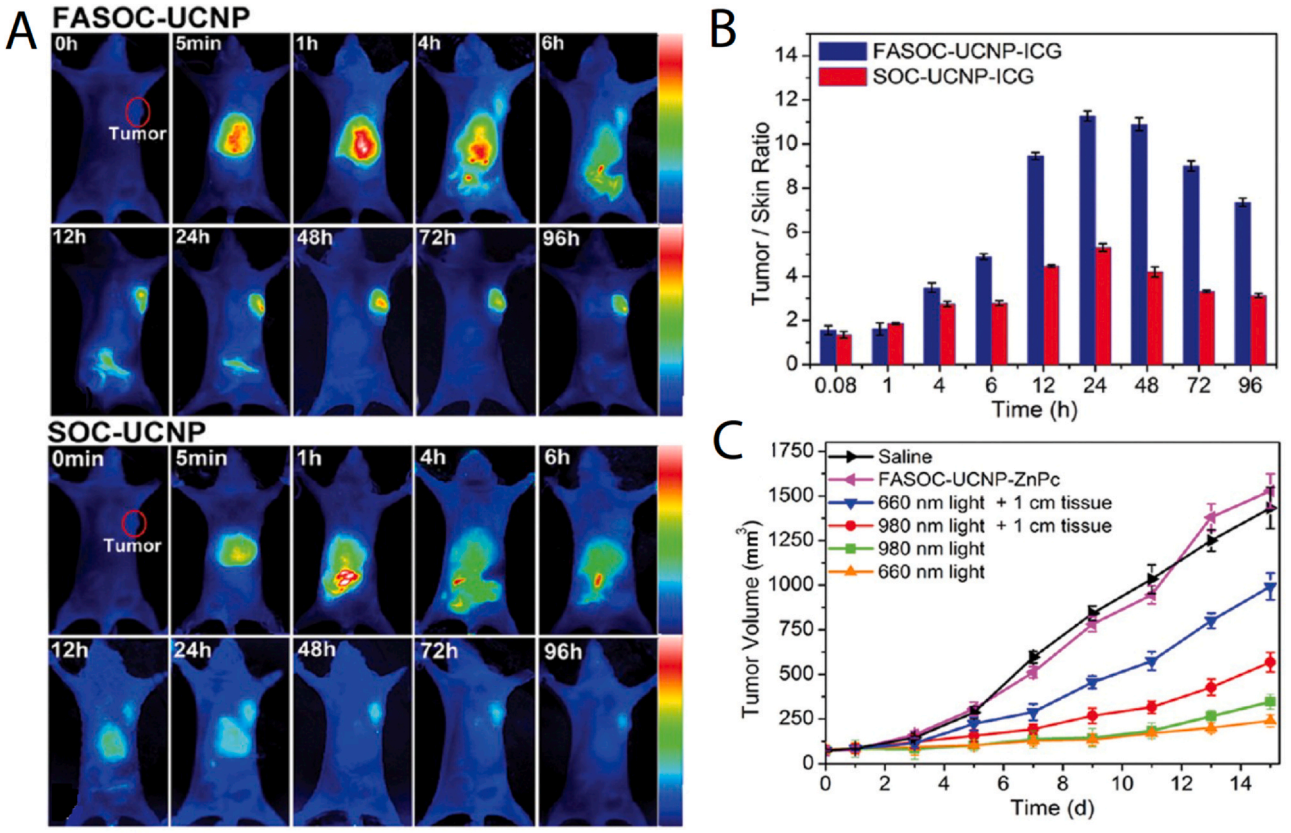

Fig. 7. (A) Fluorescence imaging of tumor bearing mice and the significant difference shown between targeted and untargeted upconverting nanoparticles (UCNPs). The nanoparticles with the targeting ligand accumulated more efficiently in the tumor. (B) Graph showing the difference between targeted and untargeted nanoconstructs in tumor-to-skin ratios of selectivity. At 24 h the ratio was 2-fold higher with targeted nanoparticles than with untargeted nanoparticles. (C) Tumor growth curves after PDT, demonstrating the difference in efficacy with respect to the depth of the tumor and the wavelength of the light used. The tumor growth of mice was most efficiently inhibited with 660 nm triggered PDT.
Adapted with permission from [87]. Copyright (2013) American Chemical Society.

PEG-modified carbon nanodots (CD) have also been functionalized with FA in order to target the ZnPc PS to FR over-expressed on HeLa cells [89]. Strong signals from the CD-PEG-FA assembly (2–8 nm) were detected in HeLa tumors, whereas no tumor signals were observed following administration of the untargeted construct (Fig. 9A). Following irradiation, the mice treated with CD-PEG-FA/ ZnPc showed notable suppression of tumor growth (Fig. 9B, C), whereas mice treated with untargeted CD-PEG/ZnPc constructs showed no significant difference than those treated with saline. Thus, the results strongly suggest that the tumor selectivity of the CD-PEG-FA/ZnPc system is negligible in the absence of molecular specificity. Specificity for FR is therefore almost entirely responsible for the construct's efficacy in tumor photodestruction. It must also be noted here that the small size of the CD-PEG-FA/ ZnPc nanoconstructs favors rapid tumor clearance of untargeted constructs, and favors the retention of targeted constructs [19]. As such, delineating the role of specificity in the tumor selective delivery of these CD-PEG-FA/ZnPc constructs becomes less challenging.

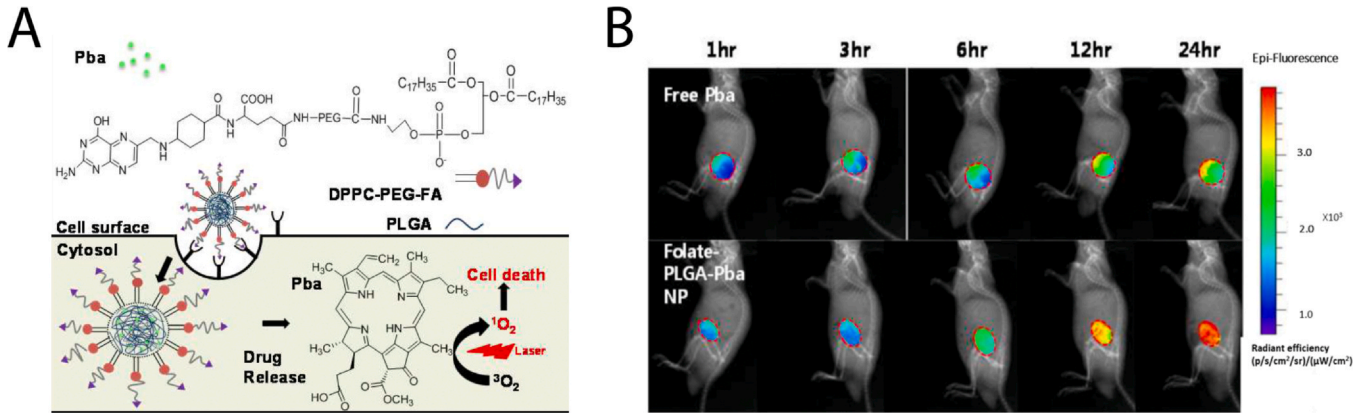

Fig. 8. (A) Schematic representation of molecular targeting with FA-PLGA-Pba nanoparticles where Pba was used as the PS and folic acid (FA) was used for targeting the folate receptor (FR) on the surface of cancer cells. (B) Fluorescence imaging showing the difference in bulk tumor delivery between targeted FA-PLGA-Pba nanoparticles and the free PS Pba. The fluorescence intensity of Pba in the tumors was highest in mice injected with the targeted FA-PLGA-Pba nanoparticles
Reprinted from [88]. Copyright (2018), with permission from Elsevier.

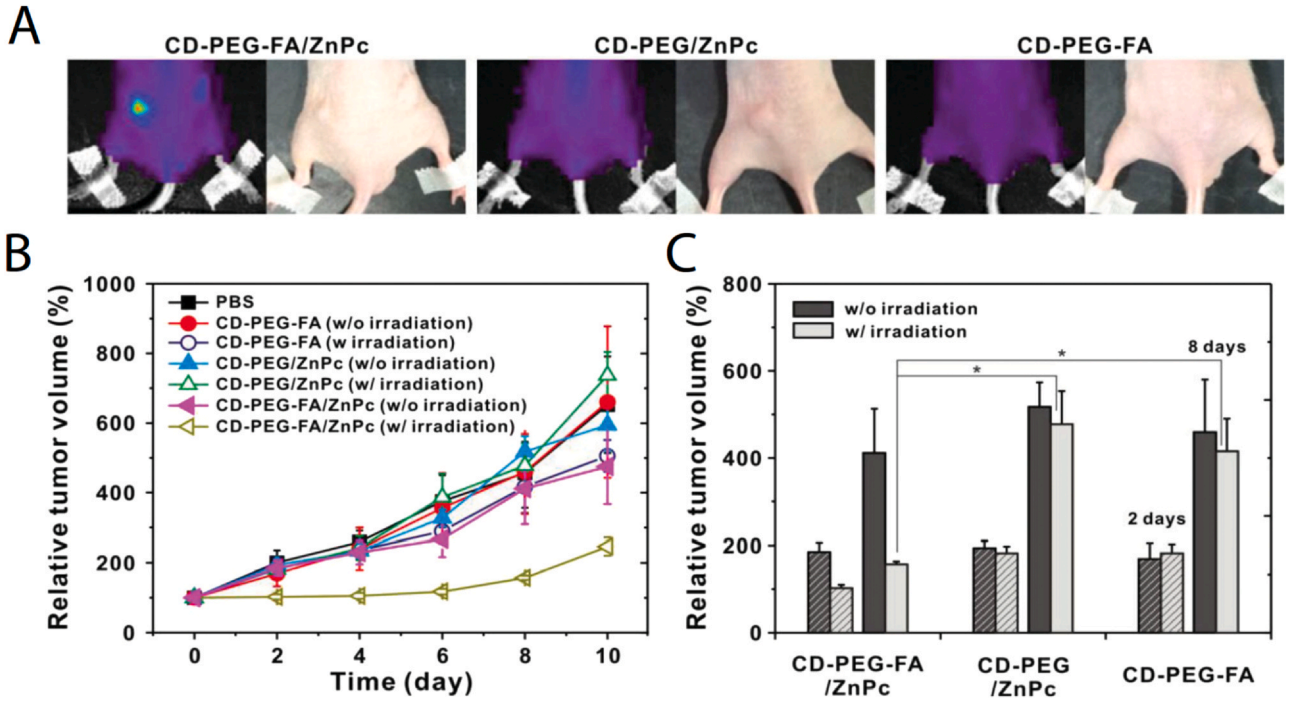

Fig. 9. (A) Fluorescence imaging of HeLa tumors in mice after 12 h of injection with Polyethylene glycol (PEG) modified carbon nanodots (CD) functionalized with Folic acid (FA) and zinc phthalocyanine (ZnPc) PS (CD-PEG-FA/ZnPc) as the targeted construct, CD-PEG/ZnPc (untargeted construct), and CD-PEG-FA (without PS). Strong fluorescence signals corresponding to the ZnPc were observed only in the group targeted with the ligand (FA). (B) Tumor growth curves from tumor bearing mice. The mice treated with CD-PEG-FA/ZnPc showed the most significant suppression of tumors. (C) Bar graph showing differences in relative tumor volumes between molecular targeted and untargeted PDT. Reproduced from [89]. Copyright 2014, with permission from John Wiley and Sons. © 2014 WILEY-VCH Verlag GmbH & Co. KGaA, Weinheim.

While the spatial localization of mt-PNMs is critical for their tumor cell-specific phototoxicity, an additional layer of control over phototoxicity can be employed by adopting aggregation-induced emission. In a recent study by Yang et al. [90], liposomes targeted with FA were used to entrap the aggregation-induced emission PSs Bis-pyrene (BP) and MC4 in a constitutively off state. Following FR specific cancer cell binding and internalization, the nanoconstructs were designed for intracellular degradation, release of the PSs in their off-state, and cytosolic PS aggregation to activate their photosensitizing properties (Fig. 10A). The MCF-7 tumor uptake of the targeted liposomes reached a maximum at 24 h following administration and photoactivation of the BP@liposomes demonstrated the most effective tumor control (Fig. 10B). The laser alone had a significant anti-tumor effect, which is likely due to photothermalization of the tumor when irradiated with the 808 nm femtosecond pulse laser using a total fluence of 2.1 kJ/cm^2 per tumor at an irradiance of 4.4 W/cm^2. Such dose parameters are typically associated with ablative photothermal therapy. Given that the PDT efficacy of untargeted constructs was not tested, it remains unclear what extent the non-specific tumor uptake, non-specific cellular internalization, and off-target aggregation-induced emission contributed to tumor control. As such, the role of specificity in an mt-PNM based on aggregation-induced emission is yet to be explored.

Another approach leveraging FR targeting was reported by Jin et al., whereby *in vivo* receptor engagement of a quenched porphysome nanostructure triggers their destabilization and recovery of fluorescence and photosensitizing activity [91]. In this approach,

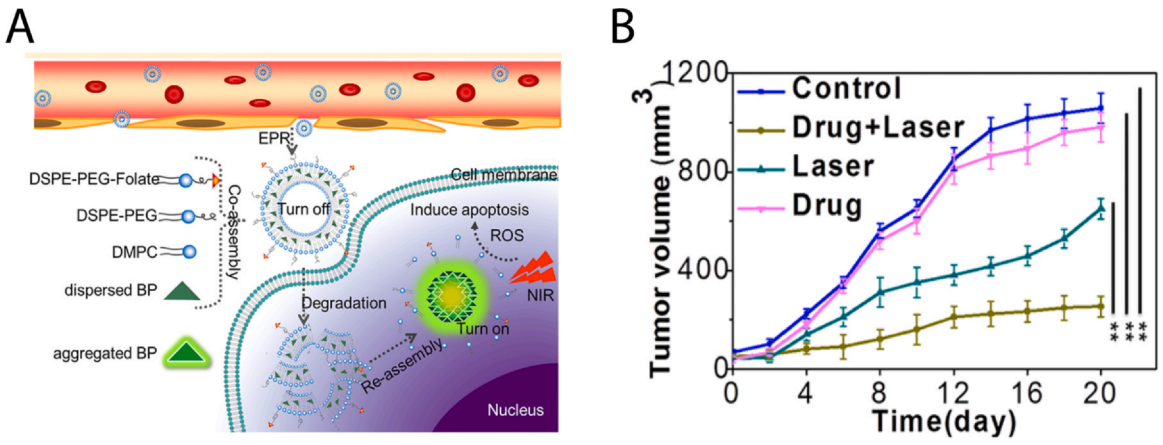

Fig. 10. (A) Schematic diagram of targeted PDT with liposome encapsulating photosensitizers, (B) Growth curve of tumor in mice after treatment with BP@liposomes only, control, laser only and BP@liposomes followed by laser. The significant suppression of the tumor was observed with the photodynamic activation of BP@liposomes (drug). Adapted with permission from [90]. Copyright (2019) American Chemical Society.

specificity was intended for both molecular targeted delivery and molecular targeted activation of the mt-PNM. Interestingly, FR targeting led to a *ca.* 2-fold compromise in KB tumor delivery (4.4% and 3.1%ID/g at 6 h and 24 h, respectively) as compared to untargeted porphysomes (8.0% and 7.5%ID/g at 6 h and 24 h, respectively). FR targeting also led to a *ca.* 2-fold decrease in tumor-to-muscle selectivity (3–4 fold for targeted, 7–8-fold for untargeted). However, specificity for FR did result in a significant activation of *in vivo* fluorescence of the porphysomes. Furthermore, specificity did impart a 7-fold reduction in KB tumor volume and extended survival following photoactivation, whereas untargeted porphysomes had no inhibitory effect on tumor growth or extended survival as compared to untreated controls. The findings here further emphasize the point that while mt-PNM specificity may even negatively impact the efficiency of tumor selective delivery, overall tumor uptake, and distribution, this does not negate the fact that their efficacy is oftentimes dictated by their recognition of and interaction with molecular targets at the cellular level [105].

Specificity using protein-based natural ligands

Other protein-based natural ligands have played a role in the development and evaluation of mt-PNMs. The natural ligand transferrin (Tf) has been used to impart transferrin receptor specificity to photocatalytic titanium dioxide (TiO_2) nanoparticles [106]. In this study, deep tissue excitation of the titanium dioxide nanoparticles was achieved through Cerenkov emission (250–600 nm) following the positron decay of the clinical positron emission tomography (PET) probe 2′-deoxy-2′-(^{18}F) fluoro-D-glucose (FDG). Titanocene, a radical photoinitiator was also incorporated into the Tf ligand. The HT1080 tumor-to-normal selectivity of the TiO_2-Tf nanoparticles was *ca* 7, whereas that of the untargeted TiO_2-PEG nanoparticles was only *ca.* 1. However, it must be noted that TiO_2-Tf nanoparticles, unlike the untargeted nanoparticles, did not contain PEG and that the hydrodynamic diameter of the untargeted TiO_2-PEG nanoparticles was 2.5-fold greater than that of the TiO_2-Tf nanoparticles. Both factors are likely to have a significant impact on the tumor selective delivery of the constructs making the interpretation of how specificity influences selectivity significantly more complex. Following intravenous administration of the TiO_2-Tf-Tc nanoparticles and the Cerenkov photon-emitting-^{18}F-FDG, HT10180 tumor growth was suppressed approximately 2-fold and survival was extended by 3-fold, as compared to untreated mice. As no direct treatment comparison between Cerenkov photon activation of TiO_2-Tf-Tc nanoparticles and untargeted TiO_2-PEG nanoparticles was made, it is unclear to what degree specificity for TR contributes to the impressive therapeutic outcomes observed *in vivo*.

Tf has also been used to target liposomes (146 nm in diameter) entrapping the PS aluminum phthalocyanine tetrasulfonate (AlPcS4) to the transferrin receptor in bladder cancer [92]. *In vitro,* a higher accumulation (fluorescence signal) of AlPcS4 was found in AY-27 cells incubated with the targeted Tf-Lip–AlPcS4 constructs than with the untargeted Lip-AlPcS4 constructs. Following PDT, cell viabilities with the targeted Tf-Lip–AlPcS4 construct was found to as low as 0.19% at 4 h but without Tf targeting the cell viability remained greater than 90%. Considering that bladder tumors are accessible by topical application, the authors instilled the constructs into the bladders of rats bearing AY-27 cell–derived bladder tumors. However, no tumor-specific accumulation of the targeted Tf-Lip–AlPcS4 constructs was observed in the tumors, which was hypothesized to be due to the presence of the glycocalyx layer. After digesting the glycocalyx with chondroitinase ABC, instillation of the targeted construct (400 μM) showed the strongest fluorescence signal arising specifically from the urothelial tumor tissue with a tumor-to-bladder ratio of 2:1. In the presence of 50 μM of competing Tf, no fluorescence was detected in the urothelial tumor, neither were PS signals detected when the untargeted construct was instilled, further confirming the specificity of the constructs *in vivo*. While preferential tumor accumulation was observed with molecular targeting, the Tf-Lip–AlPcS4 constructs did not appear to be capable of inducing significant phototoxicity. Although tumor-specific photodamage can potentially be induced by modulation of dosimetry parameters in future studies, the findings do underscore the capacity for the Tf-Lip–AlPcS4 system to exhibit true molecular specificity *in vivo,* albeit through a direct topical administration route. The findings also suggest that the paradox of binding specificity not being predictive of phototoxicity can also play a role in this system, although full dosimetry studies are required before such conclusions can be drawn.

Specificity using synthetic peptides

While globular proteins such as antibodies and protein-based natural ligands are attractive, their size can significantly alter the final mt-PNM size and surface properties, therefore drastically modifying their pharmacokinetic properties. Peptides therefore offer a particular advantage for conferring specificity onto mt-PNMs, as their decreased size and low immunogenicity reduce the effects of ligand targeting on pharmacokinetics.

In a study by Wang et al., 10 nm iron oxide (IO) nanoparticles were conjugated to fibronectin-mimetic peptide (Fmp) (Fig. 11A), which targets the tumor-associated integrin β1 receptor, and were loaded with the PS Pc4 [94]. The binding specificity of the Fmp-IO-Pc 4 nanoparticles was evaluated in head and neck squamous cell carcinoma cell lines over-expressing integrin β1 (M4E and 686LN cells) and cells with low levels of integrin β1 (M4E-15 and TU212 cells). The *in vitro* findings demonstrated that the survival of low-receptor-expressing tumor cells was greater than that of integrin β1-over-expressing cells following photoactivation. After demonstrating specificity *in vitro,* the authors evaluated the *in vivo* behavior of the Fmp-IO-Pc 4 nanoparticles in M4E tumors. Tumor-bearing mice were intravenously administered with either 0.4 mg/kg or 0.06 mg/kg of Fmp-IO-Pc 4 nanoparticles or untargeted IO-Pc 4 nanoparticles. It was found that 48 h following injection, the molecular targeted Fmp-IO-Pc 4 nanoparticles provided *ca.* 20% improvements in tumor selective delivery, as compared to the untargeted constructs. Following *in vivo* photoactivation using the injected dose of 0.4 mg/kg, both the untargeted and targeted Fmp-IO-Pc4 constructs induced the same degree of tumor control, even though tumor accumulation was higher with the targeted constructs. However, when the authors used a lower dose of 0.06 mg/kg, targeted Fmp-IO-Pc 4 nanoparticles showed significant benefit of PDT-mediated tumor control over the untargeted constructs (Fig. 11B). This particular finding on the effect of the dose administered on nanoparticle specificity is extremely important. This study shows that non-specific and untargeted nanoparticles can still effectively induce tumor photodamage given that sufficient tumor accumulation is achieved, rendering molecular targeting redundant. Although in this particular study M4E tumor uptake of the Fmp-IO-Pc4 constructs was higher with molecular targeting, the absence of an improvement in treatment efficacy when using high administered doses underscores the critical role of mt-PNM dosimetry that must be taken into consideration when attempting to delineate the effects of tumor specificity from those of the more generalized selectivity.

Although we and others have previously shown that molecular targeted gold nanoparticles are capable of receptor-specific binding and photodynamic destruction of cancer cells *in vitro* [107–109], the extent to which they bind to their target tumor cells *in vivo* has recently been questioned [110]. In the context of *in vivo* PDT, molecular targeted gold nanoparticles have been prepared by conjugating the prostate-specific membrane antigen-1 (PSMA-1) peptide ligand to PEG and then grafting it onto gold nanoparticles (AuNP) loaded with the silicon phthalocyanine PS Pc4 (Fig. 12A) [93]. The specificity of the gold nanoparticle conjugates (AuNP5kPEGPSMA-1-Pc4; 26.5 ± 1.1 nm

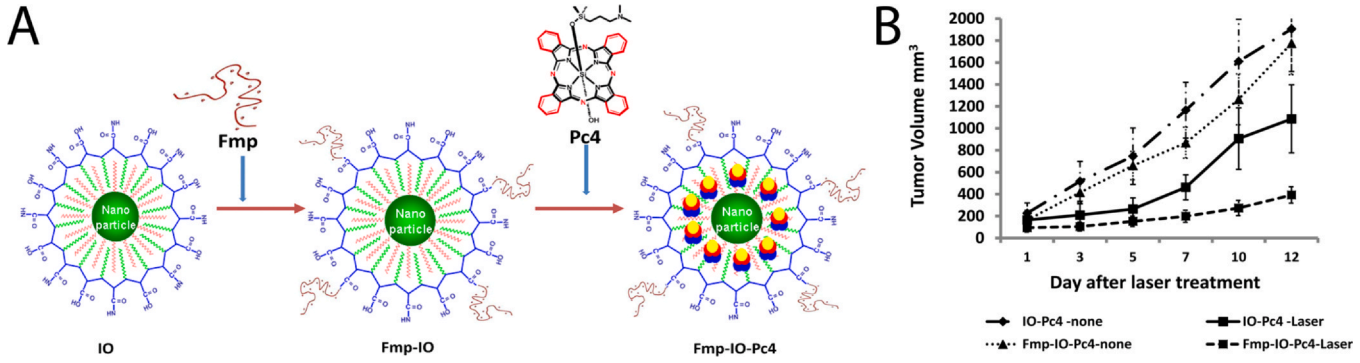

Fig. 11. (A) Schematic illustration of synthesis of Fmp-IO-Pc4 (B) Tumor growth curves after PDT using the lower dose of photosensitizer equivalent, 0.06 mg/kg. Tumor growth inhibition was most prominent in the targeted fibronectin-mimetic peptide-Iron Oxide-Pc4 (Fmp-IO-Pc4) nanoparticle group, and less so in the free Pc 4 and untargeted Iron oxide-Pc 4 (IO-Pc4) groups.
Reproduced with permission from https://pubs.acs.org/doi/10.1021/nn501652j [94]. Further permissions related to the material excerpted should be directed to the ACS.

in diameter) was initially evaluated *in vitro* in PC3pip (PSMA-positive) and PC3flu (PSMA-negative) prostate cancer cells, which demonstrated 8-fold greater photodestruction of the PC3pip (PSMA-positive) cells. *In vivo,* the AuNP5kPEG-PSMA-1-Pc4 nanoparticles exhibited 4-fold greater accumulation in PC3pip (PSMA-positive) tumors than in PC3flu (PSMA negative) tumors, demonstrating that molecular specificity of the gold nanoparticles can directly enhance the tumor selective bulk delivery in receptor-overexpressing tumors (Fig. 12B). This enhanced tumor selective bulk delivery was observed at 3 h post-injection of the constructs, whereby the gold content of excised PC3pip (PSMA-positive) tumors was *ca.* 12 μg Au per gram of tumor whilst in the PC3flu tumors, only *ca.* 3 μg Au per gram of tumor was detected. While it was concluded that PDT using the targeted constructs induced PC3pip (PSMA-positive) tumor destruction in a light dose-dependent manner, the exact impact of molecular specificity on the phototherapeutic efficacy *in vivo* remains unknown. Nonetheless, the significance of these findings is that they strongly suggest that biomolecular recognition and specificity for PSMA using this mt-PNM system directly enhances tumor selective delivery, with the potential for providing a greater degree of tumor tissue photodamage, although that remains to be investigated.

Nanographene nanoparticles (GO) carrying the PS Photochlor (HPPD) recently reported by Yu et al., have been modified with the HK peptide to specifically target cancer-associated integrin αvβ6 receptors [95]. The final targeted nanographene product (GO (HPPH)-PEG-HK; 10–100 nm in diameter) exhibited greater 4T1 tumor selective delivery than free HPPH, and more importantly, than that of the untargeted GO(HPPH)-PEG nanoparticles 24 h post-injection (Fig. 13A). Tumor selective delivery of the targeted GO (HPPH)-PEG-HK at 24 h post-injection reached an impressive *ca.* 22% ID/g, but without targeting it was significantly lower at *ca.* 14% ID/g (Fig. 13B). Thus, it can be inferred that molecular specificity for αvβ6 receptors in this study was directly responsible for *ca.* 57% enhancement in tumor selective delivery of GO(HPPH)-PEG-HK nanoconstructs. Ultimately, photoactivation of the GO(HPPH)-PEG-HK constructs were used to elicit an adaptive anti-tumor immune response against primary and metastatic disease, although the therapeutic contribution of specificity is yet to be determined.

Specificity using polysaccharides

Hyaluronic acid (HA) is a naturally occurring polysaccharide that is a major component of the extracellular matrix. HA exhibits a natural avidity for the HA receptor (CD44), which is overexpressed in a number of cancers. As such, nanoparticles formed of HA naturally exhibit specificity for the cognate tumor-associated receptor CD44, as do nanoparticles that are only surface functionalized with HA. A study by Yoon et al. described the preparation of HA nanoparticles (HANPs) incorporating the PS Ce6, through which CD44 was targeted by the inherent HA framework of the HANPs (Fig. 14A; 227.1 ± 12.5 nm diameter) [96]. The authors found that after a 30 min incubation period with Ce6-HANP, the fluorescence intensity of Ce6 was 4.1-fold higher in HT29 cells (high CD44) than in

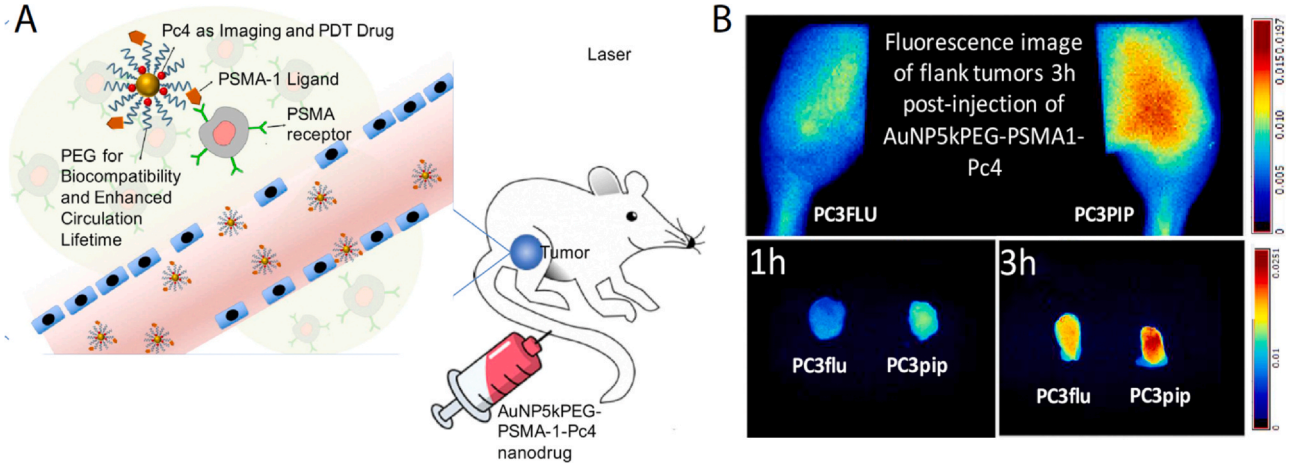

Fig. 12. (A) Schematic diagram of PDT with targeted gold nanoparticles designed for specific binding to the PSMA receptor over-expressed in prostate cancer cells. (B) Fluorescence images of PSMA receptor positive (PC3pip) and negative (PC3flu) tumors mice after administration of the targeted Pc4 PS-carrying gold nanoparticles (AuNP5kPEGPSMA-1-Pc4). Images show a higher degree of tumor accumulation of AuNP5kPEGPSMA-1-Pc4 nanoparticles in the PSMA receptor positive PC3pip tumor.
Adapted with permission from [93]. Copyright (2018) American Chemical Society.

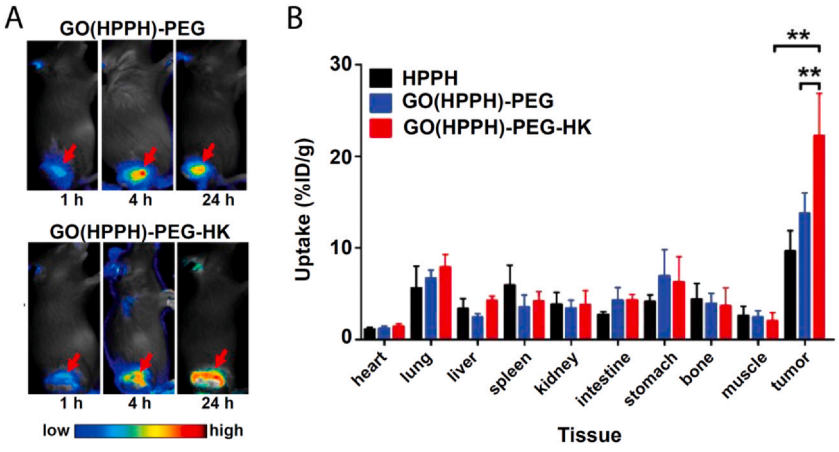

Fig. 13. (A) Fluorescence imaging of the 4T1 tumor-bearing mice with given dose of 30 nmol HPPH equivalent. At 24 h post-injection, the tumor fluorescence intensity of GO (HPPH)-PEG-HK (targeted) was significantly higher than other probes. (B) Quantification of %ID/g uptake of HPPH (photosensitizer), GO(HPPH)-PEG (untargeted) and GO(HPPH)-PEG-HK (targeted) in tumor and other organs. The uptake was significantly higher with targeted nanoparticles in tumor.
Adapted with permission from [95]. Copyright (2017) American Chemical Society.

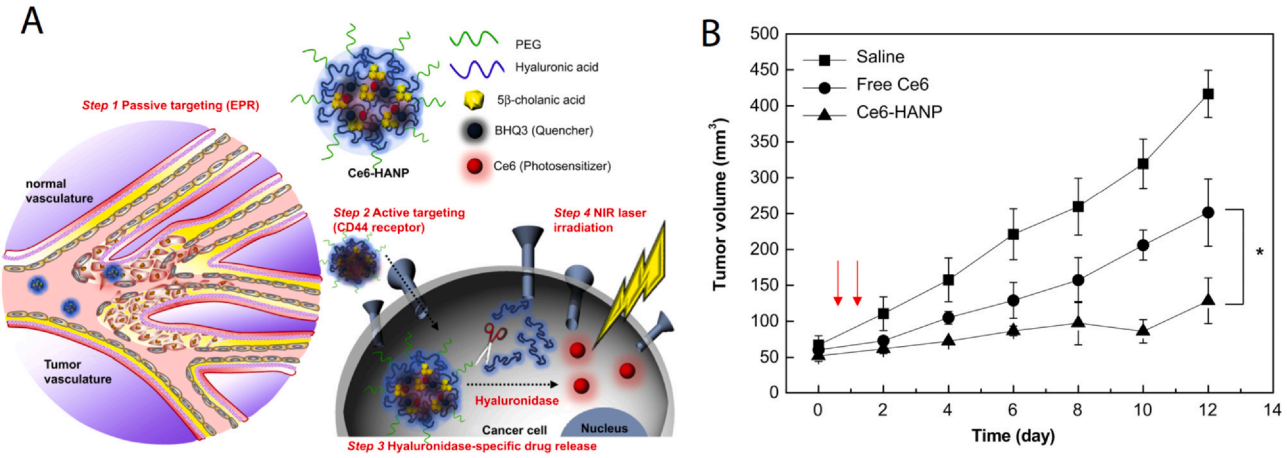

Fig. 14. (A) Schematic representation of PDT mediated by Ce6 photosensitizer-carrying hyaluronic acid nanoparticles (HANP) which target the CD44 receptor on the surface of the cancer cells. (B) HT29 tumor growth after PDT using the free Ce6 photosensitizer or the Ce6-HANPs. Tumor growth in mice treated with PDT using the Ce6-HANPs was significantly slower than tumor growth following PDT using free Ce6, and untreated control tumors.
Reprinted from [96]. Copyright (2012), with permission from Elsevier.

receptor-null NIH/3T3 cells *in vitro*. In this case, the molecular specificity of phototoxicity generally corresponded to the observed trend in binding specificity, whereby photodestruction of HT29 cells was 60% more efficient than that of NIH/3T3 following photoactivation of the Ce6-HANPs. Following PDT of HT-29 tumors *in vivo*, hemorrhagic injury was observed in the mice injected with Ce6-HANP but not in those injected with free Ce6. Although there was a significant improvement in tumor control between Ce6-HANP and free Ce6 (Fig. 14B), the hemorrhagic injury suggests a significant degree of vascular photodamage also. A prior study has also shown that CD44 is over-expressed on angiogenic endothelial cells, and treatment with anti-CD44 antibodies is capable of inducing hemorrhaging in an *in vitro* model of angiogenesis [111]. It is therefore conceivable that the Ce6-HANPs exerted molecular-specific phototoxic effects on the angiogenic endothelial cells in addition to the tumor cells. While inducing photodamage to blood vessels and tumor cells simultaneously has the potential for enhancing overall tumor responses to PDT [101,102], the direct role of molecular specificity remains ambiguous, even though efficacious in this system. This is especially the case, as the HANP nanoparticle framework itself which mediates tumor selective delivery is also the same entity that mediates tumor-associated receptor specificity.

A recent study explored the combined effect of PDT and chemotherapy using a size transforming nanosystem targeting CD44. A micelle termed ICPNM was formed from the self-assembly of cholic acid (CA), 4-carboxy-3-fluorophenylboronic acid (PBA) and a hexadecapeptide (ICP) decorated with an indocyanine green derivative (ICGD) as the PS. The nanoparticles were also loaded with the chemotherapeutic agent SN38. They were then coated with FA and dopamine-decorated HA to target FR and CD44 respectively, resulting in a 130 nm nanoparticle [97]. *In vitro* studies performed in B16 cell lines and spheroids suggested a higher degree of ICGD uptake with hICP (targeted) and ICP (untargeted) constructs than with free ICGD. Transformation of hICP NPs into small nanoparticles was found to be advantageous as it improved the internalization of the nanoparticles by the cells. In *in vivo* studies using B16 tumors, the authors found that molecular targeting of the constructs resulted in a 3-fold enhancement in tumor selectivity, a 2-fold enhancement in tumor growth control and a 5-fold increase in cure rates.

Specificity using aptamers

Aptamers are also attractive ligands for mt-PNMs due to their small size and tunable avidity for tumor-associated receptors. In addition, metal organic frameworks (MOFs) are playing an

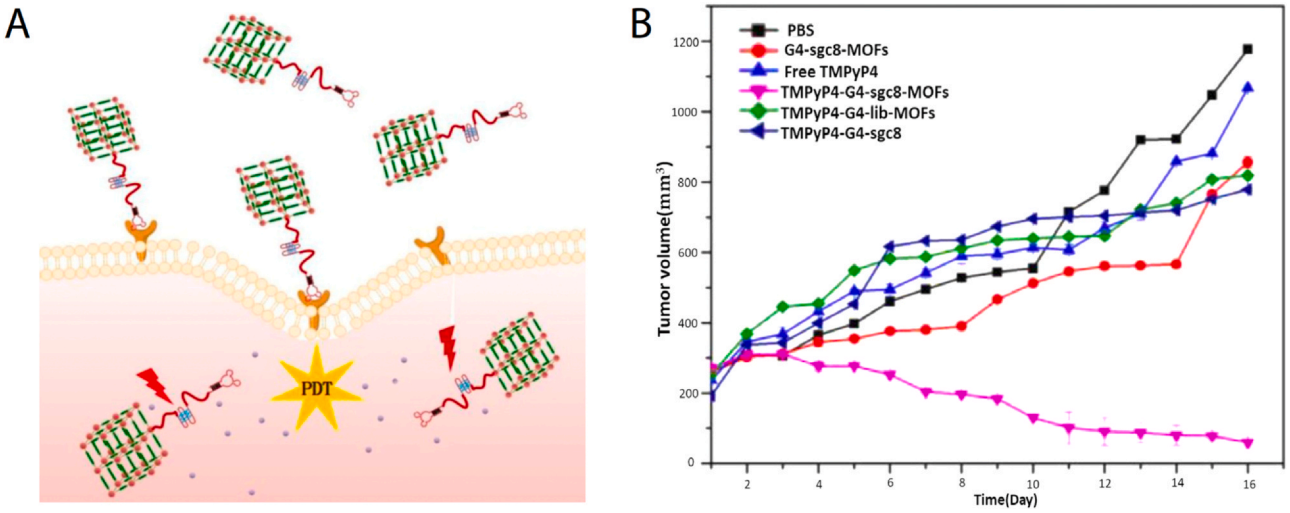

Fig. 15. (A) Schematic representation of aptamer targeted photodynamic therapy (PDT). (B) Tumor growth curves after PDT in HeLa tumor bearing mice with six test groups where a significant decrease in tumor volume was observed even after 16 days following PDT using the targeted TMPyP4-G4-sgc8-NMOF constructs. PDT using the untargeted sham TMPyP4-G4-lib-NMOF constructs had no inhibitory effect on tumor growth, corroborating the fact that specificity is critical for the observed anti-tumor efficacy of the targeted TMPyP4-G4-sgc8-NMOF mt-PNMs.
Reproduced from Meng et al. [99].

increasingly critical role in PDT, due to the fact that the simplified system, whereby the PS is the nanoparticle itself, is conducive to expedited clinical translation. In a study by Meng et al., a Zr-based nanoscale MOF (Zr-(NMOF)) system (93 nm) was targeted to the tumor-associated protein tyrosine kinase 7 (PTK7) by functionalization with the G4 aptamer, G4-sgc8 [99]. The G4-sgc8-NMOFs was also conjugated to the PS 10, 15, 20-tetrakis (1-methylpyridinium-4-yl) porphyrin (TMPyP4) (Fig. 15A). The uptake of TMPyP4-G4-sgc8-NMOFs in PTK7-overexpressing HeLa cells and CEM cells was found to be greater than in non-cancerous Ramos cells. In a highly insightful and elegant approach to delineate specificity from selectivity *in vivo*, the authors prepared sham NMOFs conjugated to an irrelevant G4-lib sequence to replace the targeting G4-sgc8 aptamer. The sham TMPyP4-G4-lib-NMOFs serve as an ideal control for the targeted TMPyP4-G4-sgc8-NMOFs as they present no alterations in the size or nature of the nanosystem. These non-specific TMPyP4-G4-lib-NMOFs exhibited low uptake in PTK7 receptor positive HeLa cells and CEM cells, further confirming the molecular specificity of the TMPyP4-G4-sgc8-NMOF system at the cellular level. The *in vitro* uptake patterns of the targeted and untargeted NMOFs were also consistent with the trends in phototoxicity. *In vivo*, HeLa tumor growth inhibition was highest for the group treated with the targeted TMPyP4-G4-sgc8-NMOFs with photoactivation, whereas the sham TMPyP4-G4-lib-NMOFs with photoactivation had no impact on tumor growth. Considering that no *in vivo* PDT efficacy was observed without molecular targeting, it can be concluded that the *in vivo* molecular specificity of the TMPyP4-G4-lib-NMOF system is predominantly responsible for its PDT efficacy, and that tumor selective delivery alone in the absence of molecular target binding, plays a negligible role. Without specific aptamer-receptor interactions, no anti-tumor efficacy can be exerted by photoirradiation of the NMOFs (Fig. 15B). However, the higher irradiance and fluence of the laser used in this study (2 W/cm^2 and 3600 J/cm^2, respectively) is typically associated with photothermal therapy. It is therefore possible that in this study, a photothermal effect also contributed to the tumor damage in addition to PDT, although that speculation must be tested. The caveat is that the photothermal effect, which has been reported for MOFs [112] has a lower spatial resolution in its thermal ablation zone than PDT's confined tissue damage, which exhibits an RMS radial diffusion distance at the nm–μm scale as described earlier. Thus, the molecular precision of targeted PDT at the boundary between tumor and healthy tissue can become compromised if the photothermal effect becomes the predominant mode of tissue damage. Furthermore, intratumoral administration of the constructs in this study confounds the interpretation of specificity and selectivity further, as treatment is only dependent on enhanced retention with vascular delivery playing no role at all.

The mt-PNM – mononuclear phagocyte system (MPS) axis

It is well established that nanoconstructs, such as PNMs and mt-PNMs, are removed from the body through the Mononuclear Phagocytic System (MPS), which comprises of bone marrow progenitors, blood monocytes and tissue macrophages. While Kupfer cells, resident liver macrophages, are the predominant mononuclear cell subtype responsible for clearing nanoconstructs from circulation, splenic marginal zone and red pulp macrophages also play a critical role [113,114]. In addition, persinal macrophages in the bone marrow and pulmonary intravascular macrophages in the lung have also been implicated in the clearance of nanoconstructs [115]. Specifically within cancer, tumor-associated macrophages (TAMs) are central to the capture, clearance and removal of nanoconstructs from the tumor interstitium. Macrophages internalize nanoparticles through complement receptor-mediated, Fc-γ receptor-mediated, and scavenger-receptor (SR) mediated phagocytosis [116]. Recognition and phagocytosis of nanoconstructs is facilitated by the protein corona which consists of opsonins such as fibrinogen, complement factor and IgG [117]. Ligand functionalization of nanoconstructs can in fact promote opsonization and macrophage uptake, especially in the case of IgG antibody functionalized nanoconstructs with exposed Fc fragments [116,118]. As such, it is critical to understand and manipulate the interplay between the physico-chemical properties of each mt-PNM system and the MPS in order to intelligently and rationally engineer more effective phototherapeutics.

Generally speaking, avoiding the MPS system is desirable in order to prolong nanoconstruct circulation in the bloodstream and increase their tumor selective delivery. However, for mt-PNMs, dosimetry is not only dependent on bulk tumor delivery, and can be compensated for by modulating the light fluence to counteract suboptimal tumor delivery as discussed earlier. This is a particularly important concept for PDT, given that molecular specificity for the tumor tissue can also be attained through an mt-PNM system. However, the MPS system, mostly in regard to TAMs, has been implicated in complex and diverse mechanisms of promoting tumor

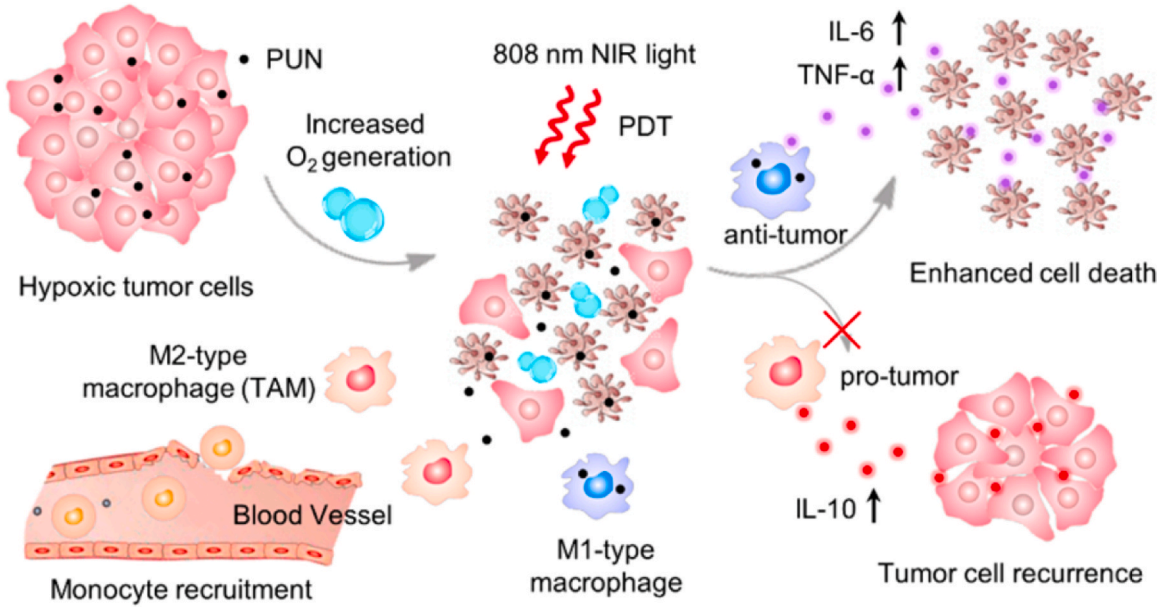

Fig. 16. Scheme of lanthanide-doped upconversion nanocrystal (UCN) photodynamic therapy polarization of tumor-associated macrophages (TAMs) from M2 to M1 phenotype using a photosensitizer-loaded UCN nanoconjugate (PUNs).
Reprinted with permission from [122]. Copyright (2018) American Chemical Society.

damage following PDT, as summarized in Fig. 17. These center on the immunomodulatory effects and anti-vascular effects of PDT when it exploits the MPS system as described in this section.

Photodynamic re-polarization of tumor-associated macrophages (TAMs) and enhancing TAM tumoricidal activity using mt-PNMs

TAMs have been shown to internalize nanoconstructs more efficiently than the tumor cells themselves [119]. Activated TAMs exist in two forms: the M2 pro-tumorigenic phenotype and the M1 anti-tumorigenic phenotype. While it may initially seem problematic that PNMs can be sequestered by TAMs, and likely even more so for ligand functionalized mt-PNMs, PDT has in fact been reported to re-polarize TAMs from the M2 pro-tumorigenic phenotype to the M1 anti-tumorigenic phenotype. Thus, it is conceivable that ligand targeting of mt-PNMs, especially those targeted by full-length antibodies with exposed Fc fragments, or other phagocytosis-promoting ligands, may in fact inadvertently promote the anti-tumor efficacy of PDT by re-polarizing the TAMs. Assuming that molecular specificity and enhanced tumor cell photodestruction is also achieved by a particular mt-PNM system, ligand targeting is likely to further augment the efficacy by re-polarizing TAMs towards the anti-tumorigenic M1 phenotype. As such, the specificity of an mt-PNM system may in fact unintentionally elicit a multi-angular assault on the tumor microenvironment by promoting both the immunomodulatory effects of PDT, in addition to tumor tissue-specific photodamage [120–122]. In addition to the re-polarization of TAMs, PDT has been shown to stimulate macrophage secretion of pro-inflammatory prostaglandin-E2 and TNF-α, increase nitric oxide production and enhance tumor cell lysis and phagocytosis by macrophages [123–126]. All of these secondary effects have the potential to directly promote tumor tissue damage if occurring in TAMs that preferentially sequester mt-PNMs [127].

One such example is a study by Ai et al. that leveraged photosensitizer-loaded lanthanide-doped upconversion nanocrystals (UCNs) with a combination of manganese dioxide (MnO_2) nanosheets and hyaluronic acid (HA), that were referred to as PUNs [122]. The authors designed the PUNs to specifically target TAMs; however, through the HA layer, CD44 receptor specificity in of itself is also capable of promoting photodamage specifically in the tumor cells and angiogenic endothelial cells, as we discussed in section *Delineating the therapeutic contributions of specificity from selectivity* of this review. This PUN construct was shown to reprogram M2 TAMs to the M1 phenotype following photoactivation using 808 nm light by producing singlet oxygen in hypoxic conditions through a reaction between MnO_2 and hydrogen peroxide in the acidic tumor microenvironment (Fig. 16). A similar effect has also been reported *in vitro* using a differentiated THP-1 monocyte cell line, whereby PDT using non-targeted temoporfin PS nanoprecipitates in water induced re-polarization of macrophages to the M1 phenotype [128].

Another study by Shi et al. leveraged the high expression of the mannose receptor (CD206) by M2 TAMs to target mannose functionalized, PEGylated PLGA nanoparticles entrapping the PS ICG in order to re-polarize TAMs towards the M1 phenotype using PDT [120]. PDT of B16 melanoma tumors *in vivo* using an 808 nm laser resulted in a significant reduction in the M2 cell population and a significant increase in the M1 population, thereby reversing the immunosuppressive nature of the tumor. Antigen presentation and T-cell priming by macrophages was also enhanced following PDT using these nanoparticles. A significant anti-tumor and anti-metastatic effect was also observed when PDT was mediated by entrapped titanium dioxide nanoparticles and Cerenkov light emitted by the decay of an FDG PET probe. While the mannose receptor expressed by M2 TAMs is emerging as a critical target for tumor photo-immunomodulation [121], it is also broadly overexpressed in tumor tissue, and has been used for molecular specific photodestruction of tumors [129]. Thus, while it may be difficult to delineate between the role of mt-PNM specificity for tumor tissue photodestruction and photo-immunomodulation, both are likely to contribute to an enhanced and multi-angled anti-tumor effect when directing mt-PNMs towards the mannose receptor.

Implications of perivascular macrophages in anti-vascular PDT

It has been reported that TAMs localize in the perivascular space within the tumor, promoting uptake of nanoconstructs before extensive tissue penetration [130]. As ligand functionalization can increase nanoconstruct uptake by TAMs, ligand targeting may result in a higher accumulation of these nanoconstructs in tumor perivascular macrophages (Fig. 17). While this may be problematic for the

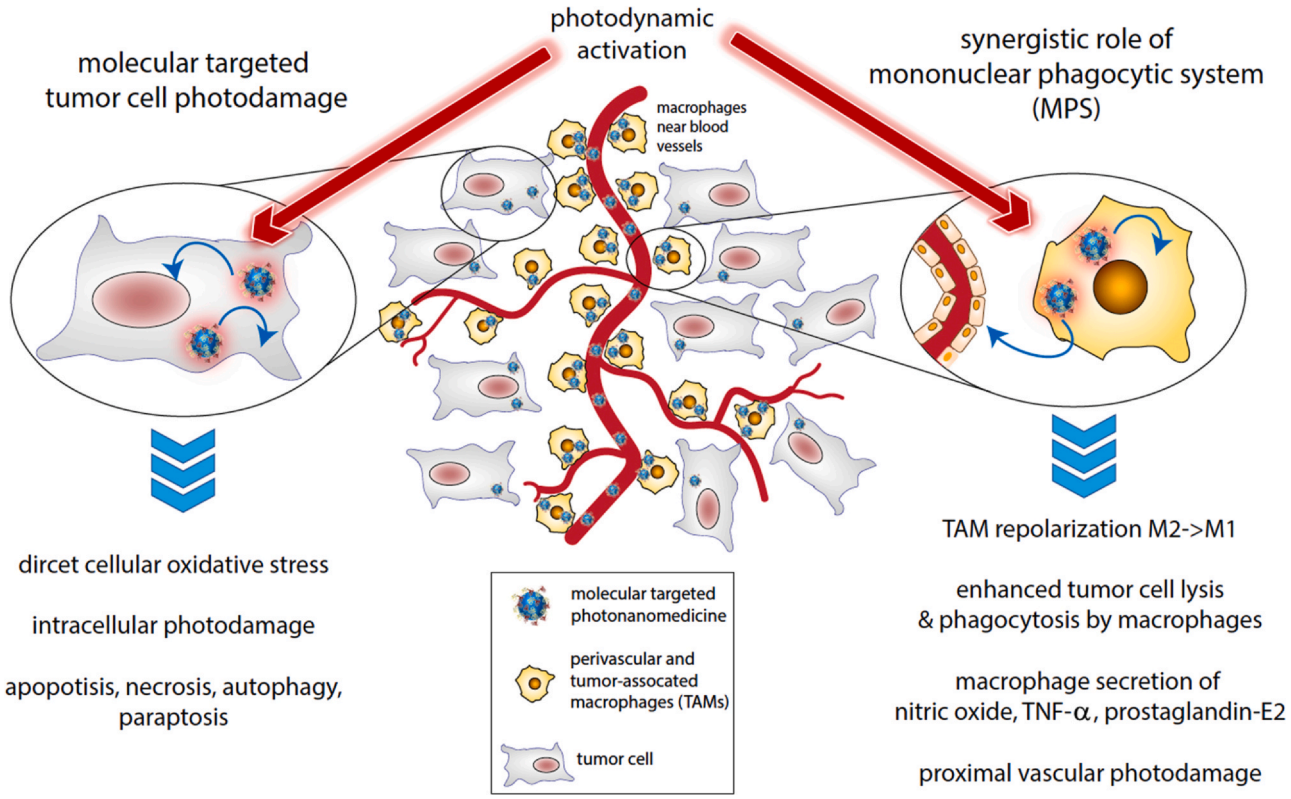

Fig. 17. Schematic representation summarizing the role of the MPS in molecular targeted PDT using mt-PNMs. In addition to direct photodamage to tumor cells, photoactivated mt-PNMs captured by perivascular macrophages and TAMs play a synergistic role in repolarizing immunosuppressive M2 TAMs to anti-tumor M1 TAMs, enhance macrophage lysis and phagocytosis of tumor cells, release of pro-inflammatory and anti-tumor factors, and potentially assisting vascular photodamage.

majority of LTNs, the distinct and multifaceted mechanisms of tumor photodamage by PDT may capitalize on this phenomenon. As discussed earlier, PDT has been found to be most effective in tumors when the PS is localized in both the tumor tissue and angiogenic blood vessels [101,102]. In addition to binding to target tumor cells, mt-PNMs are likely to be efficiently sequestered in perivascular macrophages, and thus photoactivation may inadvertently result in an augmented anti-vascular PDT effect. Again, while molecular specificity in of itself may not be the result of an augmented anti-vascular PDT effect, it is likely a secondary consequence of ligand functionalization.

Biomimetic nanoconstructs for immune evasion and homotypic targeting

Biomimetic nanoconstructs derived from cell membranes of cancer cells or otherwise, are a highly significant emerging paradigm in anti-cancer drug delivery that capitalize on two critical concepts: evasion of immune surveillance and homotypic targeting. The innate ability of cancer cells to evade immune surveillance, invade surrounding tissue and metastasize contributes to the immune evading and homotypic targeting properties of biomimetic nanoconstructs derived from cancer cell membranes. Thus, immune evasion and homotypic targeting directly mediate the capacity for biomimetic nanoconstructs to exhibit tumor tissue selectivity and tumor tissue specificity, respectively.

The MPS system is largely responsible for the removal of nanoconstructs from circulation, thereby shortening their circulation half-life, minimizing their tumor selective delivery and overall tumor tissue selectivity. As such, the immune-evading characteristics of biomimetic nanoconstructs is responsible for their enhanced tumor selectivity, as compared to more conventional nanoconstructs. The mechanisms underlying the prolonged circulation half-lives and enhanced tumor selectivity of biomimetic nanoconstructs are not fully understood. However, it has been found that CD47 expressed on 4T1 cells is a self-marker that is responsible for the prevention of macrophage uptake and facilitates immune-evasion [131]. Functionalization of nanoparticles with CD47 has in fact been shown to confer immune-evasive properties on synthetic nanoparticles to enhance their tumor selective delivery, which can also be adopted for LTNs such as mt-PNMs [132].

Homotypic targeting, also known as homologous targeting, refers to the process by which biomimetic nanoconstructs derived from cancer cell membranes exhibit a discrete molecular specificity for the parent cancer cells from which they were derived. Tumor tissue specificity resulting from homotypic recognition of biomimetic nanoconstructs has been demonstrated using a plethora of different cancer cell lines and their respective tumors [133]. Although the molecular basis of homotypic recognition of a biomimetic nanoconstruct to its respective parent tumor cell is largely unexplored, a study on 4T1 cells reported an involvement of membrane CD44 and CD326 [134]. However, the variability observed between how homotypic recognition varies considerably between cell lines suggests the involvement of significantly more complex biorecognition processes that warrant further investigation [135]. While biomimetic nanoconstructs can also be derived from the plasma membranes of other cell types including red blood cells, chimeric antigen receptor (CAR)-T cells, stem cells, macrophages, fibroblasts, and others, tumor cell specificity resulting from homotypic targeting is limited to cancer cell membrane-derived biomimetic nanoconstructs [136,137]. Tumor tissue specificity of biomimetic nanoconstructs that have not derived from cancer cell membranes can also be achieved in certain instances given that the parent cells used to prepare the biomimetic nanoconstructs have a discrete molecular

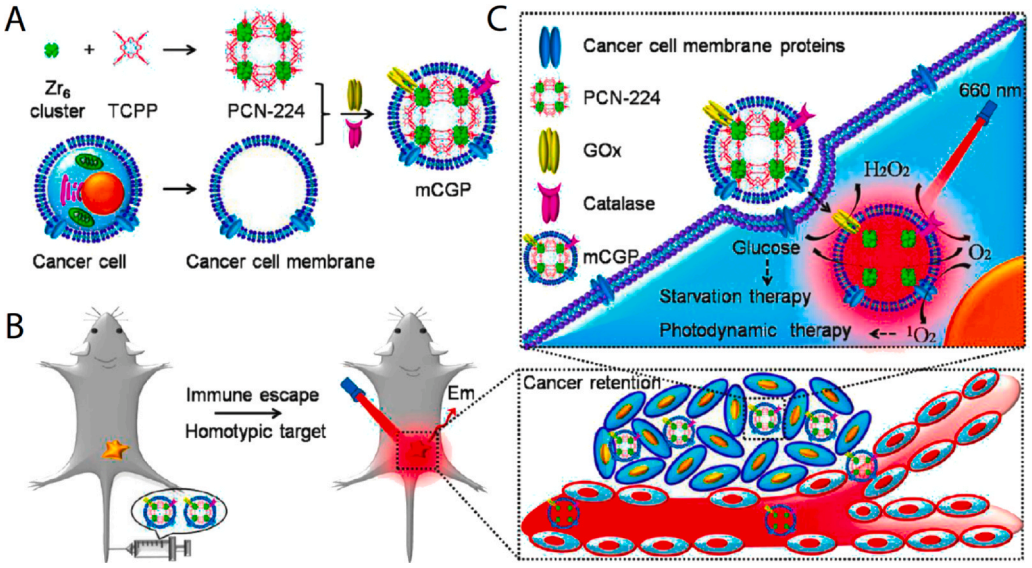

Fig. 18. Illustration of cancer cell membrane camouflaged nanoparticles, mem@catalase@GOx@PCN-224, designated as mCGP. (A) Preparation of mCGP nanoparticles. (B) Camouflaging using cancer cell membrane resulting in increased cancer accumulation after intravenous injection. (C) Reactions of mCGP are used for starvation therapy and promote $^1O_2$ generation with photodynamic therapy.
Reprinted with permission from [138]. Copyright 2017 American Chemical Society.

affinity for the tumor cells. Although the molecular basis of the tumor specificity for biomimetic nanoconstructs that have not been derived from cancer cell membranes has not been studied in detail, an elegant recent example includes CAR-T cell membrane-coated biomimetic nanoconstructs which specifically recognize and bind to GPC3 expressed on hepatocellular carcinoma cells *in vitro* and *in vivo* [137].

Biomimetic nanoparticle technology is also emerging as a powerful approach for mt-PNMs. A study by Li et al. found that nanoparticles containing the photosensitizer PCN-224 (mem@catalase@GOx@PCN-224; or mCGP, 152.8 nm in diameter) could be cloaked with 4T1 murine mammary carcinoma cell membranes to better target 4T1 cancer cells *in vitro* and *in vivo* (Fig. 18) [138]. The authors showed that PDT using free PCN-224 resulted in 67.5% tumor growth inhibition *in vivo*. However, PDT using the biomimetic mCGP nanoparticles exhibited 97.1% tumor growth inhibition; an increase they attribute to both immune evasion and homotypic targeting. While in this study, it remains unclear what the direct roles of immune evasion and homotypic targeting are on biomimetic nanoconstruct selectivity and specificity *in vivo,* the concept and the findings hold substantial promise.

In another study by Cheng et al. a zeolitic imidazolate framework (ZIF-8) nanoplatform incorporating an aluminum phthalocyanine chloride tetrasulfonic acid PS was cloaked with HeLa cancer cell membranes (Fig. 19A–C) [139]. *In vitro*, HeLa cell membrane cloaking provided a marked increase in HeLa cell phototoxicity, which was not observed in irrelevant and off-target COS7 cells. *In vivo,* HeLa cell membrane cloaking led to a two-fold longer circulation time in mice bearing HeLa tumors and a two-fold increase in tumor cell specificity, as compared to uncloaked nanoparticles. This translated to a two-fold improvement in anti-tumor PDT efficacy as compared to uncloaked nanoparticles, which can be attributed to an interplay between enhanced tumor selective delivery and molecular specificity at the cellular level.

In an elegant and highly important study on orthotopic glioma by Jia et al., biomimetic ICG-loaded nanoparticles (BLIPO-ICG) were prepared from C6 glioma cell membranes (Fig. 20A, B) [135]. Interestingly, the BLIPO-ICG provided up to *ca.* 8-fold recognition of C6 cells, as compared to other glioma cells *in vitro.* In orthotopic tumors with compromised blood-brain barriers at 14 days after implantation, the tumor selective delivery of the BLIPO-ICG was 1.8–1.9 -fold higher than that of the conventional liposomes containing ICG. At an earlier timepoint of 7 days following implantation when the blood-brain barrier was intact within the tumor, it was found that no tumor uptake of liposomal ICG was detected 12 h following administration. In contrast, at that same timepoint, the BLIPO-ICG disrupted the blood-brain barrier at the tumor site and exhibited up to 8.4-fold tumor selective delivery. It was also found that the homotypic targeting with the BLIPO-ICG improved the phototherapeutic effect in the orthotopic tumors, as compared to liposomal ICG. While the findings present substantial and unprecedented therapeutic benefits of biomimetic nanoconstructs, the smaller size of the BLIPO-ICG nanoparticles, as compared to the LIPO-ICG (104 nm verses 151 nm, respectively) may confound the comparison between the two. Nonetheless, the blood-brain-barrier permeating effects of the biomimetic nanoconstructs provide unparalleled opportunities in overcoming vascular and interstitial barriers to mt-PNM delivery, and can offer complementary routes of tumor delivery in light of the discrepancies observed with the enhanced permeability and retention effect [140].

Biomimetic drug delivery systems also include those generated from exosomes or extracellular microvesicles. A study by Lee et al. generated exosomes and extracellular microvesicles (referred to as membrane vesicles) from HeLa and CT26 cancer cells that were packaged with a zinc phthalocyanine PS using a fusogenic liposome technique [141]. The subsequent membrane vesicles were found to penetrate tumor spheroids more efficiently than liposomes packaged with the same zinc phthalocyanine, and also accumulated *ca.* 5-fold more in avascular regions of CT26 tumors than the liposomes 48 h following administration. The exosomes were also twice as effective at inducing CT26 tumor photodamage than the liposomes. *In vitro,* the membrane vesicles also exerted up to 3–5-fold specificity in homotypic targeting of the respective cancer cells they were derived from.

Biomimetic nanoconstructs prepared using red blood cell (RBC) membranes have also been reported to exhibit prolonged circulation half-lives and effective immune evasion owing to the natural long-circulating and immune cell-evading properties of the parent RBCs. While there is no molecular basis for cancer cell specificity, the prolonged circulation of RBC membrane-coated polymeric nanoparticles incorporating the PS 5,10,15,10-tetraphenylchlorin has also

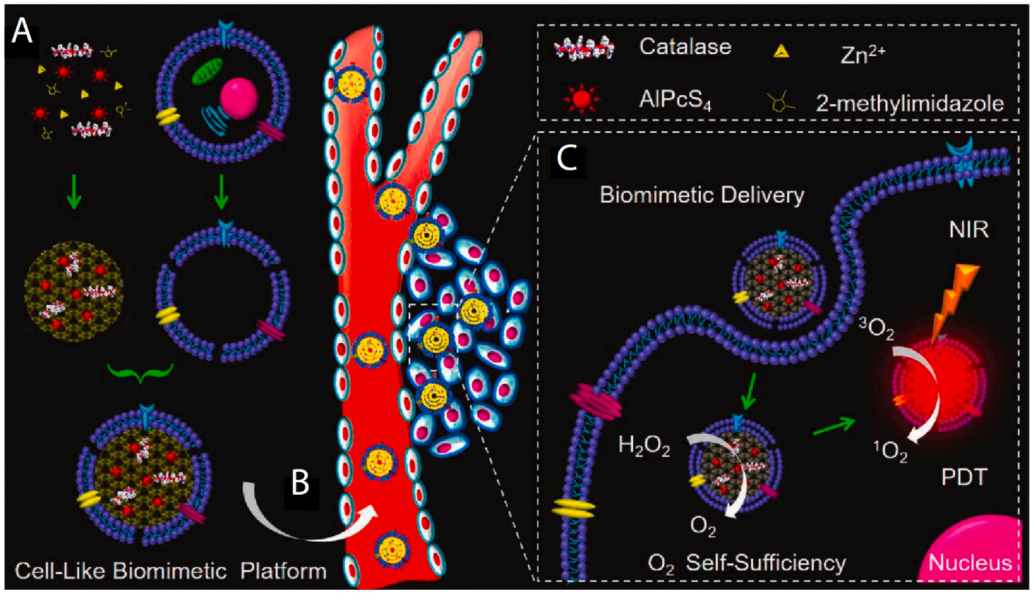

Fig. 19. Scheme of a tumor-targeting biomimetic nanoplatform composed of a zeolitic imidazolate (ZIF-8) framework, an embedded Catalase (CAT), an aluminum phthalocyanine chloride tetrasulfonic acid PS, and a HeLa cancer cell membrane (Mem), and thus was referred to as CAT-PS-ZIF@Mem. (A) Preparation process of CAT-PS-ZIF@Mem nanoplatform. (B) Accumulation of nanoplatform in tumor region after blood circulation after intravenous injection. (C) Selective PDT under NIR irradiation due to homologous targeting of the biomimetic nanoplatform.
Reprinted with permission from [139]. Copyright 2016 Wiley Online Library.

proven to be advantageous [142]. RBC membrane-coating exhibited a 4.6-fold enhancement in HeLa tumor selective delivery *in vivo*. Although unexpected, the biomimetic nanoconstructs did promote *in vitro* phototoxicity in HeLa cells, as compared to uncoated polymeric nanoparticles. These findings suggest that although no known molecular-specific interactions should exist between cancer cells and RBC membranes, they are likely to exhibit elevated levels of non-specific interactions and internalization.

Although highly complex and subject to substantial degrees of variability, the biomimetic nanoconstruct approach is of the most

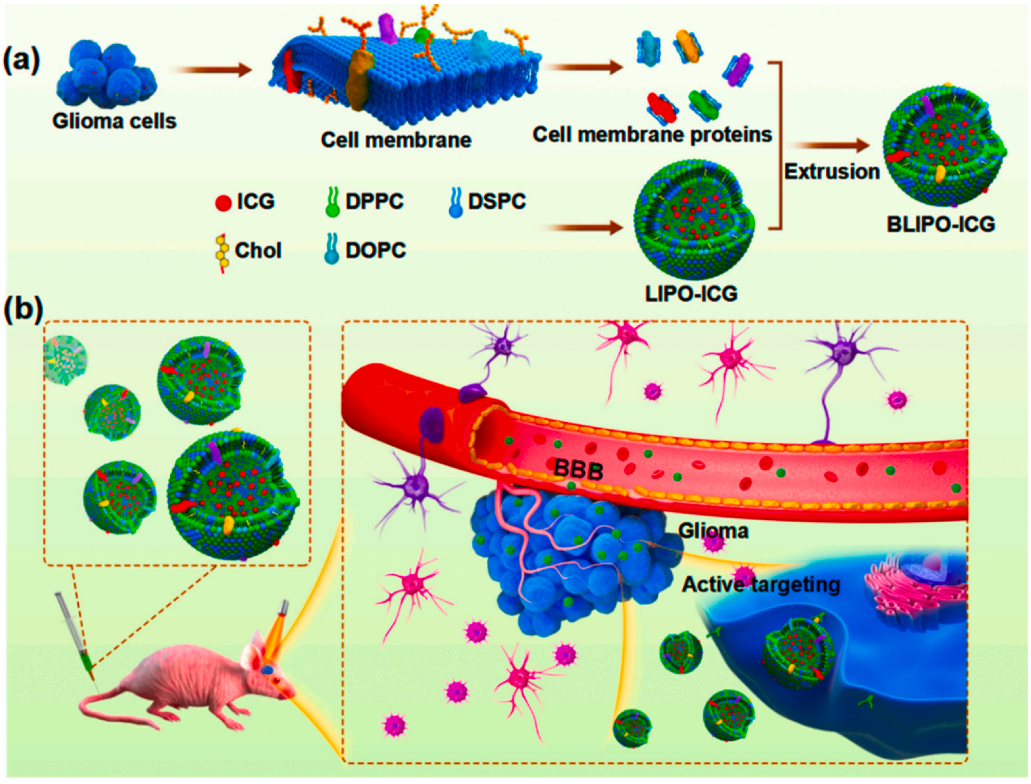

Fig. 20. Scheme of biomimetic ICG-loaded liposome (BLIPO-ICG) preparation and use with orthotopic glioma. (A) Preparation of BLIPO-ICG nanoparticles. (B) Active targeting of BLIPO-ICG and its crossing an intact Blood-Brain Barrier.
Reprinted with permission from [135]. Copyright 2019 American Chemical Society.

significant advances in patient-specific molecular targeted PDT. A deeper understanding of the molecular basis of homotypic targeting is required for clinical translation, and considerations must be made for sample purity, reproducibility and potential mutations that may diverge the phenotypic profile of the donor cells from the target cells *in vivo*.

Perspectives

Although widely used synonymously in the literature, the specificity and selectivity of ligand targeted nanomedicines (LTNs) such as molecular targeted photonanomedicines (mt-PNMs) are distinct yet interrelated phenomena. The lack of clarity between the two concepts has resulted in substantial confusion regarding the role, function and therapeutic value of the specificity of mt-PNMs if and when it exists. It is evident from the literature that the impact of the specificity of LTNs on tumor selectivity is highly variable between individual nanosystems. In addition, tumor selectivity (*i.e.* preferential tumor uptake) is oftentimes independent of the therapeutic benefit of the biomolecular recognition processes involved in tumor specificity. As mt-PNMs become increasingly complex in their constituents and multimodality, it becomes even more critical to thoroughly characterize the role of each element, in particular the targeting moiety, in order to justify its inclusion and facilitate clinical translation.

It would be remiss to emphasize the criticality of justifying ligand functionalization for clinical translation without discussing the translatability of the mt-PNM system as a whole. Multiagent mt-PNMs can provide substantial improvements in anti-tumor efficacy and treatment tolerability yet suffer from particularly complex designs. Not only must the toxicity of the individual constituents be fully evaluated both before and after integration into the mt-PNM, they must also be evaluated following phototriggered release of secondary agents in the tumor site. Phototriggered release will alter the pharmacokinetics and clearance pathways of the secondary entrapped agents and will also alter their local concentrations following photodeposition. In addition, inadvertent photodynamic priming of off-target healthy tissue will likely make it more susceptible to toxicity induced by the secondary (and tertiary) agents. Aside from special considerations regarding the mechanics of treatment induction, a useful strategy to facilitate the clinical adoption of mt-PNMs is to leverage clinically approved constituents, such as the nanoconstruct framework, activating PS molecule, secondary or tertiary agents and targeting ligands. Integration of clinically approved constituents into mt-PNMs, while advantageous, will ultimately still need to be fully evaluated as a single novel entity. Fortunately for mt-PNMs, a plethora of clinical PSs exist [143], which are compatible with a diverse armamentarium of clinical nanomedicine platforms, secondary (or tertiary) anticancer agents and viable clinical targeting molecules as discussed earlier.

The distinction between tumor selectivity and specificity requires an even clearer understanding of the biological consequences of PDT mediated by mt-PNMs, such as the immunomodulatory effects on the tumor microenvironment, the antivascular effects of PDT, and the physical modulation of the tumor parenchyma, amongst several others. This is especially the case where emerging light-based nanoparticle technologies increase in sophistication and utility including triggered agent release, synergy with secondary and tertiary therapeutics, and photoinitiated tumor-modulating biochemical cascades. Special considerations for receptor heterogeneity and vascular heterogeneity in the enhanced permeability and retention effect are also required when considering both tumor specific and tumor selective processes for mt-PNMs. While our recent work using triple-receptor targeted mt-PNMs shows that heterogeneous cancer nodules can be more efficiently destroyed *in vitro* than single-receptor targeted mt-PNMs, the impact of triple ligand functionalization on pharmacokinetics and on tumor selective delivery *in vivo* is yet to be explored [77].

Taken together, the diverse mechanisms involved in PDT and PDT-based nanotechnology using mt-PNMs have the capacity to augment tumor tissue-specific photodestruction using a multi-faceted attack that can prove to be far superior to more conventional LTNs. This however can only be achieved effectively given that mt-PNM synthesis is rational and guided by the emergent and established concepts that dictate the physiological impact of ligand functionalization. Added to that premise, adopting innovative nanotechnologies that capitalize on both tumor selectivity and tumor specificity hold substantial promise to further push the boundaries of current mt-PNM approaches. The ultimate goal of these efforts is to expedite the clinical translation of the oftentimes pronounced therapeutic benefit of mt-PNMs. Delineating between tumor selectivity and tumor specificity will undoubtedly facilitate the path to that goal by bridging the current disconnect and oftentimes misdirected efforts in approaches that improve tumor selectivity and tumor specificity, and will assist in fabricating safer and more potent anti-tumor mt-PNM regimens.

CRediT authorship contribution statement

Chanda Bhandari: Writing - Original Draft, Writing - Review & Editing. **Mina Guirguis**: Writing - Original Draft, Writing - Review & Editing. **N. Anna Savan**: Writing - Original Draft, Writing - Review & Editing. **Navadeep Shrivastava:** Writing - Review & Editing. **Sabrina Oliveira**: Conceptualization, Writing - Review & Editing. **Tayyaba Hasan**: Conceptualization. **Girgis Obaid**: Conceptualization, Investigation, Formal analysis, Writing - Original Draft, Writing - Review & Editing, Resources, Supervision, Project administration, Funding Acquisition.

Declaration of competing interest

The authors declare that they have no known competing financial interests or personal relationships that could have appeared to influence the work reported in this paper.

Acknowledgments

We thank Dr. Akilan Palanisami for insightful discussions. This work was supported by the United States of America National Institutes of Health, National Cancer Institute [K99CA215301 and R00CA215301 to G.O., and P01CA084203 and R01CA160998 to T.H.]. Financial support from the University of Texas at Dallas Startup Fund and the University of Texas STARS program to G.O. is also gratefully acknowledged.

References

[1] G. Obaid, M. Broekgaarden, A.L. Bulin, H.C. Huang, J. Kuriakose, J. Liu, T. Hasan, Photonanomedicine: a convergence of photodynamic therapy and nanotechnology, Nanoscale 8 (2016) 12471–12503.
[2] S. Tangutoori, B.Q. Spring, Z. Mai, A. Palanisami, L.B. Mensah, T. Hasan, Simultaneous delivery of cytotoxic and biologic therapeutics using nanophotoactivatable liposomes enhances treatment efficacy in a mouse model of pancreatic cancer, Nanomed. Nanotechnol. Biol. Med. 12 (2016) 223–234.
[3] S. Wang, G. Huttmann, Z. Zhang, A. Vogel, R. Birngruber, S. Tangutoori, T. Hasan, R. Rahmanzadeh, Light-controlled delivery of monoclonal antibodies for targeted photoinactivation of Ki-67, Mol. Pharm. 12 (2015) 3272–3281.
[4] B.Q. Spring, R. Bryan Sears, L.Z. Zheng, Z. Mai, R. Watanabe, M.E. Sherwood, D.A. Schoenfeld, B.W. Pogue, S.P. Pereira, E. Villa, T. Hasan, A photoactivable multi-inhibitor nanoliposome for tumour control and simultaneous inhibition of treatment escape pathways, Nat. Nanotechnol. 11 (2016) 378–387.
[5] Y. Li, Y. Deng, X. Tian, H. Ke, M. Guo, A. Zhu, T. Yang, Z. Guo, Z. Ge, X. Yang, H. Chen, Multipronged design of light-triggered nanoparticles to overcome cisplatin resistance for efficient ablation of resistant tumor, ACS Nano 9 (2015) 9626–9637.

[6] J. Liu, W. Bu, L. Pan, J. Shi, NIR-triggered anticancer drug delivery by upconverting nanoparticles with integrated azobenzene-modified mesoporous silica, Angew. Chem. Int. Ed. 52 (2013) 4375–4379.
[7] S. Hameed, P. Bhattarai, X. Liang, N. Zhang, Y. Xu, M. Chen, Z. Dai, Self-assembly of porphyrin-grafted lipid into nanoparticles encapsulating doxorubicin for synergistic chemo-photodynamic therapy and fluorescence imaging, Theranostics 8 (2018) 5501–5518.
[8] J. Xi, L. Da, C. Yang, R. Chen, L. Gao, L. Fan, J. Han, Mn^{2+}-coordinated PDA@DOX/PLGA nanoparticles as a smart theranostic agent for synergistic chemo-photothermal tumor therapy, Int. J. Nanomed. 12 (2017) 3331–3345.
[9] K.A. Carter, S. Shao, M.I. Hoopes, D. Luo, B. Ahsan, V.M. Grigoryants, W. Song, H. Huang, G. Zhang, R.K. Pandey, J. Geng, B.A. Pfeifer, C.P. Scholes, J. Ortega, M. Karttunen, J.F. Lovell, Porphyrin–phospholipid liposomes permeabilized by near-infrared light, Nat. Commun. 5 (2014) 3546.
[10] K.A. Carter, D. Luo, A. Razi, J. Geng, S. Shao, J. Ortega, J.F. Lovell, Sphingomyelin liposomes containing porphyrin-phospholipid for irinotecan chemophototherapy, Theranostics 6 (2016) 2329–2336.
[11] H. Chu, J. Zhao, Y. Mi, Z. Di, L. Li, NIR-light-mediated spatially selective triggering of anti-tumor immunity via upconversion nanoparticle-based immunodevices, Nat. Commun. 10 (2019) 2839.
[12] J. Xu, L. Xu, C. Wang, R. Yang, Q. Zhuang, X. Han, Z. Dong, W. Zhu, R. Peng, Z. Liu, Near-infrared-triggered photodynamic therapy with multitasking upconversion nanoparticles in combination with checkpoint blockade for immunotherapy of colorectal cancer, ACS Nano 11 (2017) 4463–4474.
[13] J. Li, D. Cui, J. Huang, S. He, Z. Yang, Y. Zhang, Y. Luo, K. Pu, Organic semiconducting pro-nanostimulants for near-infrared photoactivatable cancer immunotherapy, Angew. Chem. Int. Ed. 58 (2019) 12680–12687.
[14] K. Lu, C. He, N. Guo, C. Chan, K. Ni, R.R. Weichselbaum, W. Lin, Chlorin-based nanoscale metal–organic framework systemically rejects colorectal cancers via synergistic photodynamic therapy and checkpoint blockade immunotherapy, J. Am. Chem. Soc. 138 (2016) 12502–12510.
[15] L.E. Gerlowski, R.K. Jain, Microvascular permeability of normal and neoplastic tissues, Microvasc. Res. 31 (1986) 288–305.
[16] U. Prabhakar, H. Maeda, R.K. Jain, E.M. Sevick-Muraca, W. Zamboni, O.C. Farokhzad, S.T. Barry, A. Gabizon, P. Grodzinski, D.C. Blakey, Challenges and key considerations of the enhanced permeability and retention effect for nanomedicine drug delivery in oncology, Cancer Res. 73 (2013) 2412–2417.
[17] H. Maeda, K. Tsukigawa, A retrospective 30 years after discovery of the enhanced permeability and retention effect of solid tumors: next-generation chemotherapeutics and photodynamic therapy-problems, solutions, and prospects, Microcirculation 23 (2016) 173–182.
[18] S. Sindhwani, A.M. Syed, J. Ngai, B.R. Kingston, L. Maiorino, J. Rothschild, P. MacMillan, Y. Zhang, N.U. Rajesh, T. Hoang, The entry of nanoparticles into solid tumours, Nat. Mater. 19 (2020) 566–575.
[19] M.M. Schmidt, K.D. Wittrup, A modeling analysis of the effects of molecular size and binding affinity on tumor targeting, Mol. Cancer Ther. 8 (2009) 2861–2871.
[20] H. Han, M.E. Davis, Single-antibody, targeted nanoparticle delivery of camptothecin, Mol. Pharm. 10 (2013) 2558–2567.
[21] C. Mamot, D.C. Drummond, C.O. Noble, V. Kallab, Z. Guo, K. Hong, D.B. Kirpotin, J.W. Park, Epidermal growth factor receptor–targeted immunoliposomes significantly enhance the efficacy of multiple anticancer drugs in vivo, Cancer Res. 65 (2005) 11631–11638.
[22] D.W. Bartlett, H. Su, I.J. Hildebrandt, W.A. Weber, M.E. Davis, Impact of tumor-specific targeting on the biodistribution and efficacy of siRNA nanoparticles measured by multimodality in vivo imaging, Proc. Natl. Acad. Sci. 104 (2007) 15549–15554.
[23] D.B. Kirpotin, D.C. Drummond, Y. Shao, M.R. Shalaby, K. Hong, U.B. Nielsen, J.D. Marks, C.C. Benz, J.W. Park, Antibody targeting of long-circulating lipidic nanoparticles does not increase tumor localization but does increase internalization in animal models, Cancer Res. 66 (2006) 6732–6740.
[24] N. Kotagiri, G.P. Sudlow, W.J. Akers, S. Achilefu, Breaking the depth dependency of phototherapy with Cerenkov radiation and low-radiance-responsive nanophotosensitizers, Nat. Nanotechnol. 10 (2015) 370–379.
[25] R. Muchekehu, D. Liu, M. Horn, L. Campbell, J. Del Rosario, M. Bacica, H. Moskowitz, T. Osothprarop, A. Dirksen, V. Doppalapudi, A. Kaspar, S.R. Pirie-Shepherd, J. Coronella, The effect of molecular weight, PK, and valency on tumor biodistribution and efficacy of antibody-based drugs, Transl. Oncol. 6 (2013) 562–IN6.
[26] T. Saga, R.D. Neumann, T. Heya, J. Sato, S. Kinuya, N. Le, C.H. Paik, J.N. Weinstein, Targeting cancer micrometastases with monoclonal antibodies: a binding-site barrier, Proc. Natl. Acad. Sci. 92 (1995) 8999–9003.
[27] G. Obaid, B.Q. Spring, S. Bano, T. Hasan, Activatable clinical fluorophore-quencher antibody pairs as dual molecular probes for the enhanced specificity of image-guided surgery, J. Biomed. Opt. 22 (2017) 1.
[28] B.W. Pogue, E.L. Rosenthal, S. Achilefu, G.M. Van Dam, J. Biomed. Opt. 23 (2018) 100601.
[29] S.E. Miller, W.S. Tummers, N. Teraphongphom, N.S. van den Berg, A. Hasan, R.D. Ertsey, S. Nagpal, L.D. Recht, E.D. Plowey, H. Vogel, First-in-human intraoperative near-infrared fluorescence imaging of glioblastoma using cetuximab-IRDye800, J.Neuro-Oncol. 139 (2018) 135–143.
[30] K.M. Tichauer, Molecular-guided surgery: molecules, devices, and applications II, Int. Soc. Opt. Photonics (2016) 969608.
[31] H.S. Sardar, Q. Zai, X. Xu, J.R. Gunn, B.W. Pogue, K.D. Paulsen, E.R. Henderson, K.S. Samkoe, Dual-agent fluorescent labeling of soft-tissue sarcomas improves the contrast based upon targeting both interstitial and cellular components of the tumor milieu, J. Surg. Oncol. (2020) jso.26190.
[32] K.S. Samkoe, C. Wang, E. Chen, L. Tafe, K. Tichauer, Molecular-guided surgery: molecules, devices, and applications VI, Int. Soc. Opt. Photonics (2020) 112220N.
[33] J. Moan, On the diffusion length of singlet oxygen in cells and tissues, J. Photochem. Photobiol. B Biol. 6 (1990) 343–344.
[34] R. Roots, S. Okada, Estimation of life times and diffusion distances of radicals involved in X-ray-induced DNA strand breaks or killing of mammalian cells, Radiat. Res. 64 (1975) 306–320.
[35] A. Sigel, Metal ions in biological systems, Interrelations between Free Radicals and Metal Ions in Life Processes Volume 36 Routledge, 2018..
[36] C.L. Vestergaard, H. Flyvbjerg, I.M. Møller, Intracellular signaling by diffusion: can waves of hydrogen peroxide transmit intracellular information in plant cells, Front. Plant Sci. 3 (2012) 295.
[37] C.C. Winterbourn, The biological chemistry of hydrogenperoxide, Methods in Enzymology, Elsevier, 2013, pp. 3–25.
[38] C.C. Winterbourn, Reconciling the chemistry and biology of reactive oxygen species, Nat. Chem. Biol. 4 (2008) 278–286.
[39] K. Li, W. Zhang, H. Fang, W. Xie, J. Liu, M. Zheng, X. Wang, W. Wang, W. Tan, H. Cheng, Superoxide flashes reveal novel properties of mitochondrial reactive oxygen species excitability in cardiomyocytes, Biophys. J. 102 (2012) 1011–1021.
[40] L. Packer, E. Cadenas, Nitric oxide: Nitric oxide, Part E, in: Lester Packer (Ed.), Pt. E, Gulf Professional Publishing, 2005.
[41] I. Rizvi, G. Obaid, S. Bano, T. Hasan, D. Kessel, Photodynamic therapy: promoting in vitro efficacy of photodynamic therapy by liposomal formulations of a photosensitizing agent, Lasers Surg. Med. 50 (2018) 499–505.
[42] I. Rizvi, S. Nath, G. Obaid, M.K. Ruhi, K. Moore, S. Bano, D. Kessel, T. Hasan, A combination of visudyne and a lipid-anchored liposomal formulation of benzoporphyrin derivative enhances photodynamic therapy efficacy in a 3D model for ovarian cancer, Photochem. Photobiol. 95 (2019) 419–429.
[43] G. Obaid, S. Bano, S. Mallidi, M. Broekgaarden, J. Kuriakose, Z. Silber, A.L. Bulin, Y. Wang, Z. Mai, W. Jin, D. Simeone, T. Hasan, Impacting pancreatic cancer therapy in heterotypic in vitro organoids and in vivo tumors with specificity-tuned, NIR-activable photoimmunonanoconjugates: towards conquering desmoplasia, Nano Lett. 19 (2019) 7573–7587.
[44] T. Hasan, B. Ortel, A. Moor, B. Pogue, Holland-Frei Cancer Medicine, 6th edition, Decker Periodicals Publ. Incorporated, 2003.
[45] B.C. Wilson, M.S. Patterson, L. Lilge, Implicit and explicit dosimetry in photodynamic therapy: a new paradigm, Lasers Med. Sci. 12 (1997) 182–199.
[46] A.E. O'Connor, W.M. Gallagher, A.T. Byrne, Porphyrin and nonporphyrin photosensitizers in oncology: preclinical and clinical advances in photodynamic therapy, Photochem. Photobiol. 85 (2009) 1053–1074.
[47] K. Plaetzer, B. Krammer, J. Berlanda, F. Berr, T. Kiesslich, Photophysics and photochemistry of photodynamic therapy: fundamental aspects, Lasers Med. Sci. 24 (2009) 259–268.
[48] V.V. Tuchin, Light scattering study of tissues, Physics-Uspekhi 40 (1997) 495–515.
[49] A.N. Bashkatov, E.A. Genina, V.I. Kochubey, V. Rubtsov, E.A. Kolesnikova, V.V. Tuchin, Optical properties of human colon tissues in the 350 – 2500 nm spectral range, Quantum Electron. 44 (2014) 779–784.
[50] C. Ash, M. Dubec, K. Donne, T. Bashford, Effect of wavelength and beam width on penetration in light-tissue interaction using computational methods, Lasers Med. Sci. 32 (2017) 1909–1918.
[51] A. Bashkatov, E. Genina, V. Kochubey, V. Tuchin, Optical properties of human skin, subcutaneous and mucous tissues in the wavelength range from 400 to 2000 nm, J. Phys. D Appl. Phys. 38 (2005) 2543–2555.
[52] P. O'Mahoney, M. Khazova, M. Higlett, T. Lister, S. Ibbotson, E. Eadie, Use of illuminance as a guide to effective light delivery during daylight photodynamic therapy in the U.K, Br. J. Dermatol. 176 (2017) 1607–1616.
[53] A.L.R. de Souza, K. Marra, J. Gunn, K.S. Samkoe, S.C. Kanick, S.C. Davis, M.S. Chapman, E.V. Maytin, T. Hasan, B.W. Pogue, Comparing desferrioxamine and light fractionation enhancement of ALA-PpIX photodynamic therapy in skin cancer, Br. J. Cancer 115 (2016) 805–813.
[54] U. Kaw, M. Ilyas, T. Bullock, L. Rittwage, M. Riha, A. Vidimos, B. Hu, C.B. Warren, E.V. Maytin, A regimen to minimize pain during blue light photodynamic therapy of actinic keratoses: bilaterally controlled, randomized trial of simultaneous versus conventional illumination, J. Am. Acad. Dermatol. 82 (2020) 862–868.
[55] S. Monro, K.L. Colón, H. Yin, J. Roque III, P. Konda, S. Gujar, R.P. Thummel, L. Lilge, C.G. Cameron, S.A. McFarland, Transition metal complexes and photodynamic therapy from a tumor-centered approach: challenges, opportunities, and highlights from the development of TLD1433, Chem. Rev. 119 (2018) 797–828.
[56] S.L. Jacques, Optical properties of biological tissues: a review, Phys. Med. Biol. 58 (2013) R37–R61.
[57] A. Becker, C. Hessenius, K. Licha, B. Ebert, U. Sukowski, W. Semmler, B. Wiedenmann, C. Grötzinger, Receptor-targeted optical imaging of tumors with near-infrared fluorescent ligands, Nat. Biotechnol. 19 (2001) 327–331.
[58] R. Weissleder, A clearer vision for in vivo imaging, Nat. Biotechnol. 19 (2001) 316–317.
[59] D.E. Hudson, D.O. Hudson, J.M. Wininger, B.D. Richardson, Penetration of laser light at 808 and 980 nm in bovine tissue samples, Photomed. Laser Surg. 31 (2013) 163–168.
[60] S. Mallidi, S. Anbil, A.-L. Bulin, G. Obaid, M. Ichikawa, T. Hasan, Beyond the barriers of light penetration: strategies, perspectives and possibilities for photodynamic therapy, Theranostics 6 (2016) 2458–2487.

[61] P. Agostinis, K. Berg, K.A. Cengel, T.H. Foster, A.W. Girotti, S.O. Gollnick, S.M. Hahn, M.R. Hamblin, A. Juzeniene, D. Kessel, M. Korbelik, J. Moan, P. Mroz, D. Nowis, J. Piette, B.C. Wilson, J. Golab, Photodynamic therapy of cancer: an update, CA Cancer J. Clin. 61 (2011) 250–281.
[62] G. Obaid, W. Jin, S. Bano, D. Kessel, T. Hasan, Nanolipid formulations of benzoporphyrin derivative: exploring the dependence of nanoconstruct photophysics and photochemistry on their therapeutic index in ovarian cancer cells, Photochem. Photobiol. 95 (2019) 364–377.
[63] Y. Shen, A.J. Shuhendler, D. Ye, J.-J. Xu, H.-Y. Chen, Two-photon excitation nanoparticles for photodynamic therapy, Chem. Soc. Rev. 45 (2016) 6725–6741.
[64] B. Liu, C. Li, P. Yang, Z. Hou, J. Lin, 808-nm-Light-excited lanthanide-doped nanoparticles: rational design, luminescence control and theranostic applications, Adv. Mater. 29 (2017) 1605434.
[65] H. Qiu, M. Tan, T.Y. Ohulchanskyy, J.F. Lovell, G. Chen, Nanomaterials (2018) 344.
[66] Q.Q. Dou, C.P. Teng, E. Ye, X.J. Loh, Blockade of oral tolerance to ovalbumin in mice by silver nanoparticles, Nanomedicine 10 (2015) 419–431.
[67] Y. Shen, A.J. Shuhendler, D. Ye, J.J. Xu, H.Y. Chen, Two-photon excitation nanoparticles for photodynamic therapy, Chem. Soc. Rev. 45 (2016) 6725–6741.
[68] W. Peng, H.S. de Bruijn, E. Farrell, M. Sioud, V. Mashayekhi, S. Oliveira, G.M. van Dam, J.L.N. Roodenburg, M.J.H. Witjes, D.J. Robinson, Epidermal growth factor receptor (EGFR) density may not be the only determinant for the efficacy of EGFR-targeted photoimmunotherapy in human head and neck cancer cell lines, Lasers Surg. Med. 50 (2018) 513–522.
[69] E. Driehuis, S. Spelier, I. Beltran Hernandez, R. de Bree, S.M. Willems, H. Clevers, S. Oliveira, Patient-derived head and neck cancer organoids recapitulate EGFR expression levels of respective tissues and are responsive to EGFR-targeted photodynamic therapy, J. Clin. Med. 8 (2019) 1880.
[70] A.P. Castano, T.N. Demidova, M.R. Hamblin, Mechanisms in photodynamic therapy: part one—photosensitizers, photochemistry and cellular localization, Photodiagn. Photodyn. Ther. 1 (2004) 279–293.
[71] A.P. Castano, T.N. Demidova, M.R. Hamblin, Mechanisms in photodynamic therapy: part two—cellular signaling, cell metabolism and modes of cell death, Photodiagn. Photodyn. Ther. 2 (2005) 1–23.
[72] J.P. Celli, B.Q. Spring, I. Rizvi, C.L. Evans, K.S. Samkoe, S. Verma, B.W. Pogue, T. Hasan, Imaging and photodynamic therapy: mechanisms, monitoring, and optimization, Chem. Rev. 110 (2010) 2795–2838.
[73] P. Foroozandeh, A.A. Aziz, Insight into cellular uptake and intracellular trafficking of nanoparticles, Nanoscale Res. Lett. 13 (2018) 339.
[74] L.J. Pike, Growth factor receptors, lipid rafts and caveolae: an evolving story, Biochim. Biophys. Acta (BBA) Mol. Cell Res. 1746 (2005) 260–273.
[75] G.J. Doherty, H.T. McMahon, Mechanisms of endocytosis, Annu. Rev. Biochem. 78 (2009) 857–902.
[76] S. Zhang, H. Gao, G. Bao, Physical principles of nanoparticle cellular endocytosis, ACS Nano 9 (2015) 8655–8671.
[77] S. Bano, G. Obaid, J. Swain, M. Yamada, B.W. Pogue, K. Wang, T. Hasan, NIR photodynamic destruction of PDAC and HNSCC nodules using triple-receptor-targeted photoimmuno-nanoconjugates: targeting heterogeneity in cancer, J. Clin. Med. 9 (2020) 2390.
[78] S. Wilhelm, A.J. Tavares, Q. Dai, S. Ohta, J. Audet, H.F. Dvorak, W.C. Chan, Nat. Rev. Mater. 1 (2016) 1–12.
[79] Y.-H. Cheng, C. He, J.E. Riviere, N.A. Monteiro-Riviere, Z. Lin, Meta-analysis of nanoparticle delivery to tumors using a physiologically based pharmacokinetic modeling and simulation approach, ACS Nano 14 (2020) 3075–3095.
[80] J.W. Snyder, W.R. Greco, D.A. Bellnier, L. Vaughan, B.W. Henderson, Cancer Res. 63 (2003) 8126–8131.
[81] H.C. Huang, I. Rizvi, J. Liu, S. Anbil, A. Kalra, H. Lee, Y. Baglo, N. Paz, D. Hayden, S. Pereira, B.W. Pogue, J. Fitzgerald, T. Hasan, Photodynamic priming mitigates chemotherapeutic selection pressures and improves drug delivery, Cancer Res. 78 (2018) 558–571.
[82] G. Obaid, S. Bano, S. Mallidi, M. Broekgaarden, J. Kuriakose, Z. Silber, A.L. Bulin, Y. Wang, Z. Mai, W. Jin, D. Simeone, T. Hasan, Impacting pancreatic cancer therapy in heterotypic in vitro organoids and in vivo tumors with specificity-tuned, NIR-activable photoimmunonanoconjugates: towards conquering desmoplasia, Nano Lett. 19 (2019) 7573–7587.
[83] M. Overchuk, G. Zheng, Overcoming obstacles in the tumor microenvironment: recent advancements in nanoparticle delivery for cancer theranostics, Biomaterials 156 (2018) 217–237.
[84] K. Samkoe, G. Obaid, K. Tichauer, S. Bano, Y. Park, Z. Silber, S. Hodge, S. Callaghan, M. Guirguis, S. Mallidi, B. Pogue, T. Hasan, Nano Res. (2020).
[85] Y. Liu, L. Scrivano, J.D. Peterson, M. Fens, I.B. Hernandez, B. Mesquita, J.S. Torano, W.E. Hennink, C.F. van Nostrum, S. Oliveira, EGFR-targeted nanobody functionalized polymeric micelles loaded with mTHPC for selective photodynamic therapy, Mol. Pharm. 17 (2020) 1276–1292.
[86] H. Li, C. Liu, Y.P. Zeng, Y.H. Hao, J.W. Huang, Z.Y. Yang, R. Li, Chemical strategies for enhancing activity and charge transfer in ultrathin Pt nanowires immobilized onto nanotube supports for the oxygen reduction reaction, ACS Appl. Mater. Interfaces 8 (2016) 34280–34294.
[87] S. Cui, D. Yin, Y. Chen, Y. Di, H. Chen, Y. Ma, S. Achilefu, Y. Gu, In vivo targeted deep-tissue photodynamic therapy based on near-infrared light triggered upconversion nanoconstruct, ACS Nano 7 (2013) 676–688.
[88] J. Son, S.M. Yang, G. Yi, Y.J. Roh, H. Park, J.M. Park, M.G. Choi, H. Koo, Folate-modified PLGA nanoparticles for tumor-targeted delivery of pheophorbide a in vivo, Biochem. Biophys. Res. Commun. 498 (2018) 523–528.
[89] Y. Choi, S. Kim, M.-H. Choi, S.-R. Ryoo, J. Park, D.-H. Min, B.-S. Kim, Highly biocompatible carbon nanodots for simultaneous bioimaging and targeted photodynamic therapy in vitro and in vivo, Adv. Funct. Mater. 24 (2014) 5781–5789.
[90] Y. Yang, L. Wang, H. Cao, Q. Li, Y. Li, M. Han, H. Wang, J. Li, Photodynamic therapy with liposomes encapsulating photosensitizers with aggregation-induced emission, Nano Lett. 19 (2019) 1821–1826.
[91] C.S. Jin, L. Cui, F. Wang, J. Chen, G. Zheng, Targeting-triggered porphysome nanostructure disruption for activatable photodynamic therapy, Adv. Healthc. Mater. 3 (2014) 1240–1249.
[92] A.S.L. Derycke, A. Kamuhabwa, A. Gijsens, T. Roskams, D. De Vos, A. Kasran, J. Huwyler, L. Missiaen, P.A.M. de Witte, Transferrin-conjugated liposome targeting of photosensitizer AlPcS4 to rat bladder carcinoma cells, JNCI J. Natl. Cancer Inst. 96 (2004) 1620–1630.
[93] J.D. Mangadlao, X. Wang, C. McCleese, M. Escamilla, G. Ramamurthy, Z. Wang, M. Govande, J.P. Basilion, C. Burda, Prostate-specific membrane antigen targeted gold nanoparticles for theranostics of prostate cancer, ACS Nano 12 (2018) 3714–3725.
[94] D. Wang, B. Fei, L.V. Halig, X. Qin, Z. Hu, H. Xu, Y.A. Wang, Z. Chen, S. Kim, D.M. Shin, Targeted iron-oxide nanoparticle for photodynamic therapy and imaging of head and neck cancer, ACS Nano 8 (2014) 6620–6632.
[95] X. Yu, D. Gao, L. Gao, J. Lai, C. Zhang, Y. Zhao, L. Zhong, B. Jia, F. Wang, X. Chen, Z. Liu, Inhibiting metastasis and preventing tumor relapse by triggering host immunity with tumor-targeted photodynamic therapy using photosensitizer-loaded functional nanographenes, ACS Nano 11 (2017) 10147–10158.
[96] H.Y. Yoon, H. Koo, K.Y. Choi, S.J. Lee, K. Kim, I.C. Kwon, J.F. Leary, K. Park, S.H. Yuk, J.H. Park, K. Choi, Tumor-targeting hyaluronic acid nanoparticles for photodynamic imaging and therapy, Biomaterials 33 (2012) 3980–3989.
[97] Z. Cong, L. Zhang, S.Q. Ma, K.S. Lam, F.F. Yang, Y.H. Liao, Size-transformable hyaluronan stacked self-assembling peptide nanoparticles for improved transcellular tumor penetration and photo–chemo combination therapy, ACS Nano 14 (2020) 1958–1970.
[98] T. Yin, P. Huang, G. Gao, J.G. Shapter, Y. Shen, R. Sun, C. Yue, C. Zhang, Y. Liu, S. Zhou, D. Cui, Superparamagnetic Fe3O4-PEG2K-FA@Ce6 nanoprobes for in vivo dual-mode imaging and targeted photodynamic therapy, Sci. Rep. 6 (2016) 36187.
[99] H.-M. Meng, X.-X. Hu, G.-Z. Kong, C. Yang, T. Fu, Z.-H. Li, X.-B. Zhang, Aptamer-functionalized nanoscale metal-organic frameworks for targeted photodynamic therapy, Theranostics 8 (2018) 4332–4344.
[100] J. Shen, Y. Hu, K.S. Putt, S. Singhal, H. Han, D.W. Visscher, L.M. Murphy, P.S. Low, Assessment of folate receptor alpha and beta expression in selection of lung and pancreatic cancer patients for receptor targeted therapies, Oncotarget 9 (2018) 4485–4495.
[101] S. Mallidi, K. Watanabe, D. Timerman, D. Schoenfeld, T. Hasan, Prediction of tumor recurrence and therapy monitoring using ultrasound-guided photoacoustic imaging, Theranostics 5 (2015) 289–301.
[102] B. Chen, B.W. Pogue, P.J. Hoopes, T. Hasan, Combining vascular and cellular targeting regimens enhances the efficacy of photodynamic therapy, Int. J. Radiat. Oncol. Biol. Phys. 61 (2005) 1216–1226.
[103] M. García-Díaz, S. Nonell, Á. Villanueva, J.C. Stockert, M. Cañete, A. Casadó, M. Mora, M.L. Sagristá, Do folate-receptor targeted liposomal photosensitizers enhance photodynamic therapy selectivity, Biochim. Biophys. Acta (BBA) Biomembr. 1808 (2011) 1063–1071.
[104] F. Moret, D. Scheglmann, E. Reddi, Folate-targeted PEGylated liposomes improve the selectivity of PDT with meta-tetra(hydroxyphenyl)chlorin (m-THPC), Photochem. Photobiol. Sci. 12 (2013) 823–834.
[105] P. van Driel, M.C. Boonstra, M.D. Slooter, R. Heukers, M.A. Stammes, T.J.A. Snoeks, H.S. de Bruijn, P.J. van Diest, A.L. Vahrmeijer, P.M.P. van Bergen En Henegouwen, C.J.H. van de Velde, C. Lowik, D.J. Robinson, S. Oliveira, EGFR targeted nanobody–photosensitizer conjugates for photodynamic therapy in a pre-clinical model of head and neck cancer, J. Controll. Release 229 (2016) 93–105.
[106] N. Kotagiri, G.P. Sudlow, W.J. Akers, S. Achilefu, Breaking the depth dependency of phototherapy with Cerenkov radiation and low-radiance-responsive nanophotosensitizers, Nat. Nanotechnol. 10 (2015) 370–379.
[107] T. Stuchinskaya, M. Moreno, M.J. Cook, D.R. Edwards, D.A. Russell, Targeted photodynamic therapy of breast cancer cells using antibody–phthalocyanine–gold nanoparticle conjugates, Photochem. Photobiol. Sci. 10 (2011) 822–831.
[108] G. Obaid, I. Chambrier, M.J. Cook, D.A. Russell, Targeting the oncofetal Thomsen-Friedenreich disaccharide using jacalin-PEG phthalocyanine gold nanoparticles for photodynamic cancer therapy, Angew. Chem. Int. Ed. 51 (2012) 6158–6162.
[109] G. Obaid, I. Chambrier, M.J. Cook, D.A. Russell, Cancer targeting with biomolecules: a comparative study of photodynamic therapy efficacy using antibody or lectin conjugated phthalocyanine-PEG gold nanoparticles, Photochem. Photobiol. Sci. 14 (2015) 737–747.
[110] Q. Dai, S. Wilhelm, D. Ding, A.M. Syed, S. Sindhwani, Y. Zhang, Y.Y. Chen, P. MacMillan, W.C. Chan, Quantifying the ligand-coated nanoparticle delivery to cancer cells in solid tumors, ACS Nano 12 (2018) 8423–8435.
[111] G. Cao, R.C. Savani, M. Fehrenbach, C. Lyons, L. Zhang, G. Coukos, H.M. Delisser, Involvement of endothelial CD44 during in vivo angiogenesis, Am. J. Pathol. 169 (2006) 325–336.
[112] K. Zhang, X. Meng, Y. Cao, Z. Yang, H. Dong, Y. Zhang, H. Lu, Z. Shi, X. Zhang, Metal-organic framework nanoshuttle for synergistic photodynamic and low-temperature photothermal therapy, Adv. Funct. Mater. 28 (2018) 1804634.

[113] E. Sadauskas, H. Wallin, M. Stoltenberg, U. Vogel, P. Doering, A. Larsen, G. Danscher, Kupffer cells are central in the removal of nanoparticles from the organism, Part Fibre Toxicol. 4 (2007) 10.
[114] M. Cataldi, C. Vigliotti, T. Mosca, M. Cammarota, D. Capone, Emerging role of the spleen in the pharmacokinetics of monoclonal antibodies, nanoparticles and exosomes, Int. J. Mol. Sci. 18 (2017) 1249.
[115] D. Boraschi, P. Italiani, R. Palomba, P. Decuzzi, A. Duschl, B. Fadeel, S.M. Moghimi, Nanoparticles and innate immunity: new perspectives on host defence, Semin. Immunol. 34 (2017) 33–51.
[116] C. Passirani, G. Barratt, J.P. Devissaguet, D. Labarre, Interactions of nanoparticles bearing heparin or dextran covalently bound to poly(methyl methacrylate) with the complement system, Life Sci. 62 (1998) 775–785.
[117] D.E. Owens 3rd, N.A. Peppas, Opsonization, biodistribution, and pharmacokinetics of polymeric nanoparticles, Int. J. Pharm. 307 (2006) 93–102.
[118] J.A. Harding, C.M. Engbers, M.S. Newman, N.I. Goldstein, S. Zalipsky, Immunogenicity and pharmacokinetic attributes of poly(ethylene glycol)-grafted immunoliposomes, Biochim. Biophys. Acta (BBA) Biomembr. 1327 (1997) 181–192.
[119] M.A. Miller, S. Gadde, C. Pfirschke, C. Engblom, M.M. Sprachman, R.H. Kohler, K.S. Yang, A.M. Laughney, G. Wojtkiewicz, N. Kamaly, Predicting therapeutic nanomedicine efficacy using a companion magnetic resonance imaging nanoparticle, Sci. Transl. Med. 7 (2015) 314ra183-314ra183.
[120] C. Shi, T. Liu, Z. Guo, R. Zhuang, X. Zhang, X. Chen, Reprogramming tumor-associated macrophages by nanoparticle-based reactive oxygen species photogeneration, Nano Lett. 18 (2018) 7330–7342.
[121] A.K. Azad, M.V. Rajaram, L.S. Schlesinger, J. Cytol. Mol. Biol. 1 (2014).
[122] X. Ai, M. Hu, Z. Wang, L. Lyu, W. Zhang, J. Li, H. Yang, J. Lin, B. Xing, Enhanced cellular ablation by attenuating hypoxia status and reprogramming tumor-associated macrophages via NIR light-responsive upconversion nanocrystals, Bioconjug. Chem. 29 (2018) 928–938.
[123] M. Korbelik, G. Krosl, Enhanced macrophage cytotoxicity against tumor cells treated with photodynamic therapy, Photochem. Photobiol. 60 (1994) 497–502.
[124] S. Evans, W. Matthews, R. Perry, D. Fraker, J. Norton, H.I. Pass, Effect of photodynamic therapy on tumor necrosis factor production by murine macrophages, J. Natl. Cancer Inst. 82 (1990) 34–39.
[125] B.W. Henderson, J.M. Donovan, Cancer Res. 49 (1989) 6896–6900.
[126] N. Yamamoto, T.W. Sery, J.K. Hoober, N.P. Willett, D.D. Lindsay, Effectiveness of photofrin II in aciwation of macrophages and in vitro killing of retinoblastoma cells, Photochem. Photobiol. 60 (1994) 160–164.
[127] S. Coutier, L. Bezdetnaya, S. Marchal, V. Melnikova, I. Belitchenko, J. Merlin, F. Guillemin, Foscan® (mTHPC) photosensitized macrophage activation: enhancement of phagocytosis, nitric oxide release and tumour necrosis factor-α-mediated cytolytic activity, Br. J. Cancer 81 (1999) 37–42.
[128] Z. Zhu, C. Scalfi-Happ, A. Ryabova, S. Grafe, A. Wiehe, R.U. Peter, V. Loschenov, R. Steiner, R. Wittig, Photodynamic activity of temoporfin nanoparticles induces a shift to the M1-like phenotype in M2-polarized macrophages, J. Photochem. Photobiol. B Biol. 185 (2018) 215–222.
[129] M. Gary-Bobo, Y. Mir, C. Rouxel, D. Brevet, I. Basile, M. Maynadier, O. Vaillant, O. Mongin, M. Blanchard-Desce, A. Morere, M. Garcia, J.O. Durand, L. Raehm, Mannose-functionalized mesoporous silica nanoparticles for efficient two-photon photodynamic therapy of solid tumors, Angew. Chem. Int. Ed. 50 (2011) 11425–11429.
[130] Q. Dai, S. Wilhelm, D. Ding, A.M. Syed, S. Sindhwani, Y. Zhang, Y.Y. Chen, P. MacMillan, W.C.W. Chan, Quantifying the ligand-coated nanoparticle delivery to cancer cells in solid tumors, ACS Nano 12 (2018) 8423–8435.
[131] P.L. Rodriguez, T. Harada, D.A. Christian, D.A. Pantano, R.K. Tsai, D.E. Discher, Minimal "self" peptides that inhibit phagocytic clearance and enhance delivery of nanoparticles, Science 339 (2013) 971–975.
[132] Y. Qie, H. Yuan, C.A. von Roemeling, Y. Chen, X. Liu, K.D. Shih, J.A. Knight, H.W. Tun, R.E. Wharen, W. Jiang, B.Y. Kim, Erratum: corrigendum: surface modification of nanoparticles enables selective evasion of phagocytic clearance by distinct macrophage phenotypes, Sci. Rep. 6 (2016) 30663.
[133] M. Xuan, J. Shao, J. Li, Cell membrane-covered nanoparticles as biomaterials, Natl. Sci. Rev. 6 (2019) 551–561.
[134] A. Franca, P. Aggarwal, E.V. Barsov, S.V. Kozlov, M.A. Dobrovolskaia, A. Gonzalez-Fernandez, Macrophage scavenger receptor A mediates the uptake of gold colloids by macrophagesin vitro, Nanomedicine 6 (2011) 1175–1188.
[135] Y. Jia, X. Wang, D. Hu, P. Wang, Q. Liu, X. Zhang, J. Jiang, X. Liu, Z. Sheng, B. Liu, Phototheranostics: active targeting of orthotopic glioma using biomimetic proteolipid nanoparticles, ACS Nano 13 (2018) 386–398.
[136] T. Li, X. Qin, Y. Li, X. Shen, S. Li, H. Yang, C. Wu, C. Zheng, J. Zhu, F. You, Y. Liu, Cell membrane coated-biomimetic nanoplatforms toward cancer theranostics, Front. Bioeng. Biotechnol. 8 (2020) 371.
[137] W. Ma, D. Zhu, J. Li, X. Chen, W. Xie, X. Jiang, L. Wu, G. Wang, Y. Xiao, Z. Liu, F. Wang, A. Li, D. Shao, W. Dong, W. Liu, Y. Yuan, Coating biomimetic nanoparticles with chimeric antigen receptor T cell-membrane provides high specificity for hepatocellular carcinoma photothermal therapy treatment, Theranostics 10 (2020) 1281–1295.
[138] S.Y. Li, H. Cheng, B.R. Xie, W.X. Qiu, J.Y. Zeng, C.X. Li, S.S. Wan, L. Zhang, W.L. Liu, X.Z. Zhang, Cancer cell membrane camouflaged cascade bioreactor for cancer targeted starvation and photodynamic therapy, ACS Nano 11 (2017) 7006–7018.
[139] H. Cheng, J.Y. Zhu, S.Y. Li, J.Y. Zeng, Q. Lei, K.W. Chen, C. Zhang, X.Z. Zhang, An O2 self-sufficient biomimetic nanoplatform for highly specific and efficient photodynamic therapy, Adv. Funct. Mater. 26 (2016) 7847–7860.
[140] S. Sindhwani, A.M. Syed, J. Ngai, B.R. Kingston, L. Maiorino, J. Rothschild, P. MacMillan, Y. Zhang, N.U. Rajesh, T. Hoang, Nat. Mater. (2020) 1–10.
[141] J. Lee, J. Kim, M. Jeong, H. Lee, U. Goh, H. Kim, B. Kim, J.H. Park, Liposome-based engineering of cells to package hydrophobic compounds in membrane vesicles for tumor penetration, Nano Lett. 15 (2015) 2938–2944.
[142] Q. Pei, X. Hu, X. Zheng, S. Liu, Y. Li, X. Jing, Z. Xie, Light-activatable red blood cell membrane-camouflaged dimeric prodrug nanoparticles for synergistic photodynamic/chemotherapy, ACS Nano 12 (2018) 1630–1641.
[143] H. Abrahamse, M.R. Hamblin, New photosensitizers for photodynamic therapy, Biochem. J. 473 (2016) 347–364.

Chanda Bhandari is pursuing a Ph.D. in Bioengineering at the University of Texas at Dallas under the direction of Dr. Girgis Obaid. Her present research focuses on molecular targeted nanotherapy in cancer. She received her B.E. degree in Biomedical Engineering from Purbanchal University, Nepal where she worked to develop a novel surgical glue from nanoparticles and natural materials.

Mina Guirguis is an undergraduate student working in Dr. Girgis Obaid's group at the University of Texas at Dallas. He is pursuing a B.S. in Biology and Healthcare Management and is ultimately interested in a career in medicine, where he hopes to pursue both clinical practice and research.

N. Anna Savan is currently a postbaccalaureate research fellow at the National Cancer Institute, National Institutes of Health in Bethesda, Maryland. She graduated from Michigan State University with a degree in chemistry. Her research interests involve nanoparticle drug delivery systems and cancer therapies. Her work at Michigan State was focused on breast cancer stem cells and drug delivery systems that target breast cancer metastases. Currently, she is working on drug discovery for multiple myeloma. She hopes to continue her education to learn more about drug discovery and delivery for cancer therapy.

Navadeep Shrivastava, Ph.D. is a Post-Doctoral Research Associate in the research team of Dr. Girgis Obaid at the University of Texas at Dallas. He has expertize in the synthesis of hybrid nanomaterials, nanophotonics, thermal therapy and optical nanothermometry. Currently his research is focused in nanomaterials-based molecular imaging and therapeutics. He obtained his Ph.D. in Physics (Condensed Matter Physics) on the development of hybrid nanomaterials at the Universidade Federal do Maranhão, São Luís, Brazil in 2017.

Sabrina Oliveira, Ph.D. is an Associate Professor at Utrecht University with a shared position between division of Cell Biology, Neurobiology and Biophysics, department of Biology and the division of Pharmaceutics, department of Pharmaceutical Sciences. Her current research is focused on development and evaluation of improved therapies that are directed to relevant molecular targets. She worked as a postdoc at University Medical Center Utrecht on the development of tracers based on nanobodies for optical molecular imaging. She received her Ph.D. degree on Targeted Cancer Therapies from Utrecht University obtaining an individual doctoral grant from the Portuguese Foundation for Science and Technology.

Tayyaba Hasan, Ph.D. is a Professor of Dermatology at the Wellman Center for Photomedicine, Massachusetts General Hospital and Harvard Medical School, and a Professor of Dermatology at the Harvard-Massachusetts Institute of Technology Health Sciences and Technology joint program. Her research is focused on photodynamic therapy-based approaches for the treatment and diagnosis of disease. Her research is funded by the National Institutes of Health through a Program Project grant, several individual R01 grants, a UH2/UH3 grant and an Academic-Industrial Partnership grant. She has been awarded with number of honors including the 2015 International Photodynamic Association Lifetime Achievement Award.

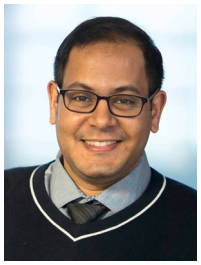

Girgis Obaid, Ph.D. is a National Cancer Institute K99/R00 funded Assistant Professor of Bioengineering at the University of Texas at Dallas. Girgis obtained his Ph.D. in Chemistry at the University of East Anglia, Norwich (U.K.) Girgis' expertize is focused on ligand functionalized nanomedicines for molecular targeted cancer therapy, including photodynamic therapy. His postdoctoral research fellowship at the Wellman Center for Photomedicine, Massachusetts General Hospital and Harvard Medical School focused on molecular targeted NIR photoactivable combination therapies for cancer. The current interests of Girgis' research group revolve around optical molecular imaging-informed nanoengineering for personalized cancer nanotherapeutics.